Dissertationes Forestales 134

Mechanisms affecting the structure and properties of heat-treated and high-temperature dried Norway spruce (*Picea abies*) wood

Marc Borrega
School of Forest Sciences
Faculty of Science and Forestry
University of Eastern Finland

Academic dissertation

To be presented, with the permission of the Faculty of Science and Forestry of the University of Eastern Finland, for public criticism in the Auditorium BOR 100 of the School of Forest Sciences, Yliopistokatu 7, Joensuu, on 11th of November 2011, at 12 o'clock noon.

Title of dissertation: Mechanisms affecting the structure and properties of heat-treated and high-temperature dried Norway spruce (*Picea abies*) wood

Author: Marc Borrega

Dissertationes Forestales 134

Thesis Supervisor:
Professor Petri P. Kärenlampi
School of Forest Sciences, University of Eastern Finland, Finland

Pre-examiners:
Associate Professor Eiichi Obataya
Graduate School of Life and Environmental Sciences, Tsukuba University, Japan
Professor Callum Hill
Forest Products Research Institute, Edinburgh Napier University, Scottland, UK

Opponent:
Professor Nasko Terziev
Swedish University of Agricultural Sciences, Sweden

ISSN 1795-7389
ISBN 978-951-651-358-7 (PDF)

(2011)

Publishers:
Finnish Society of Forest Science
Finnish Forest Research Institute
Faculty of Agriculture and Forestry of the University of Helsinki
School of Forest Sciences of the University of Eastern Finland

Editorial Office:
The Finnish Society of Forest Science
P.O. Box 18, FI-01301 Vantaa, Finalnd
http://www.metla.fi/dissertationes

Borrega, M. 2011. Mechanisms affecting the structure and properties of heat-treated and high-temperature dried Norway spruce (*Picea abies*) wood. Dissertationes Forestales 134. 52 p. Available at:
http://www.metla.fi/dissertationes/df134.htm

ABSTRACT

Wood is a natural polymeric material widely used in construction, joinery, furniture, *etc*. Many applications of wood require that the material is previously dried to a defined level below the fibre saturation point. During drying, the structure and properties of wood are modified. The objective of this research was to investigate the mechanisms that occur during drying, and to evaluate their effects on the structure and properties of wood. Understanding the effects of such mechanisms may provide a basis for developing wood drying methods that improve the performance of dried wood products.

According to the results, prolonged exposure of wood to elevated temperatures caused thermal degradation of its structural components. Temperature levels for thermal degradation considerably decreased when wood was heated in moist conditions, as in wood drying. Mass loss due to thermal degradation impaired the mechanical properties and reduced the hygroscopicity of wood. The hygroscopicity was further reduced by the irreversible hydrogen bonding (hornification) that occurred within the wood structure during drying. Increasing drying severity enhanced the occurrence of hornification. There appeared to be competing effects between mass loss and hornification in terms of the strength and stiffness of the wood.

Microscopic damage due to anisotropic drying shrinkage of cell wall layers may be minimized by conducting a slow high-temperature drying process. However, any benefits on the mechanical properties of wood induced by stress relaxation during slow high-temperature drying appeared to be offset by thermal degradation of structural components. Enhancing the mechanical performance of dried wood might be achieved by conducting a rapid high-temperature drying process up to high dryness, thus avoiding thermal degradation whilst favouring hornification. Additionally, the decreased hygroscopicity of wood may improve other physical properties such as dimensional stability.

Irreversible hydrogen bonding during high-temperature drying was manifested through the closure of macropores in the earlywood. Stress relaxation during slow high-temperature drying appeared to decrease the extent of microcracks in the earlywood, resulting in a lower nonfreezing water (NFW) content. The NFW content in wood was found to be lower than previously indicated, considering the effect of phase change on the heat capacity of water.

Keywords: differential scanning calorimetry, drying damage, hornification, hygroscopicity, mechanical properties, stress relaxation, thermal degradation, thermoporosimetry

ACKNOWLEDGEMENTS

This work was conducted at the School of Forest Sciences of the University of Eastern Finland (previously Faculty of Forest Sciences of the University of Joensuu) under the supervision of Professor Petri Kärenlampi. The decision to pursue doctoral studies was realized at the end of 2003, although due to funding difficulties, the actual work did not start until June 2005. I would like to express my sincere gratitude to Prof. Kärenlampi for believing in me and for the fruitful and interesting discussions we have had over the years. I never left his office without having learnt something new, and any signs of a scientist to be found in me are due to him. Once again, thanks Petri!

I would also like to thank my unofficial co-supervisor, Dr. Henrik Heräjarvi, at the Finnish Forest Research Institute in Joensuu, for his constant interest in my research and for always being ready to help. His positive energy has been contagious and inspiring. The pre-examiners of this thesis, Assoc. Prof. Eiichi Obataya and Prof. Callum Hill, are thanked for the valuable comments and suggestions to improve the quality of the present work.

I gratefully acknowledge the financial support provided by the Finnish Cultural Foundation, the North Karelia Regional Fund of the Finnish Cultural Foundation, the School of Forest Sciences of the University of Eastern Finland and the Niemi Foundation. I also acknowledge the Graduate School of Forest Sciences for the travelling grant awarded.

I am indebted to many people who have contributed to the completion of this thesis. Ms. Maini Mononen is thanked for helping with laboratory- and equipment-related issues. Mr. Jelle van der Beek and Mr. Jarmo Penala are thanked for helping harvesting the sample trees. I thank Mr. Keijo Silfsten, at the North Karelia University of Applied Sciences, for sawing the wooden boards. Mr. Jelle van der Beek is also thanked for helping preparing wood specimens for thermal treatments and high-temperature drying experiments. Ms. Reeta Stöd and Mr. Hannu Koivunen, at the Finnish Forest Research Institute, kindly arranged the preparation of wood specimens for mechanical testing in the radial direction. Prof. Leila Alvila, at the Department of Chemistry of the University of Eastern Finland, is thanked for her support and advice with the differential scanning calorimeter. Dr. Dennis Jones is acknowledged for the language revision of the summary of this thesis. My current colleagues, at the Department of Forest Products Technology of Aalto University, are thanked for their encouragement to finish my doctoral studies. Special thanks go to all my friends in Joensuu and in Helsinki for the good times we have had together.

Finally, I would like to thank my parents, Goyo and Anna, and my brother Xavier, for their endless love, trust and support in everything I have ever attempted in life. You have always been an amazing example to me. And you, my loved Raisa, thank you for standing by me throughout the years, encouraging me during the downs and sharing with me the ups of this long process. This all started because of you!

Helsinki, September 2011

Marc Borrega

LIST OF ORIGINAL ARTICLES

This thesis is a summary of the following articles, which are referred to in the text by the Roman numerals I-VI. All articles are reprinted with the kind permission of the publishers.

I Borrega, M. and Kärenlampi, P.P. Effect of relative humidity on thermal degradation of Norway spruce (*Picea abies*) wood. 2008. Journal of Wood Science 54(4):323-328.
doi 10.1007/s10086-008-0953-9

II Borrega, M. and Kärenlampi, P.P. Hygroscopicity of heat-treated Norway spruce (*Picea abies*) wood. 2010. European Journal of Wood and Wood Products 68(2):233-235.
doi 10.1007/s00107-009-0371-8

III Borrega, M. and Kärenlampi, P.P. Mechanical behavior of heat-treated spruce (*Picea abies*) wood at constant moisture content and ambient humidity. 2008. Holz als Roh-und Werkstoff 66(1):63-69.
doi 10.1007/s00107-007-0207-3

IV Borrega, M. and Kärenlampi, P.P. Three mechanisms affecting the mechanical properties of spruce wood dried at high temperatures. 2010. Journal of Wood Science 56(2):87-94.
doi 10.1007/s10086-009-1076-7

V Borrega, M. and Kärenlampi, P.P. Radial mechanical properties of high-temperature dried Norway spruce (*Picea abies*) wood. 2011. Wood Material Science and Engineering 6(3):147-154.
doi 10.1080/17480272.2011.561017

VI Borrega, M. and Kärenlampi, P.P. Cell wall porosity in Norway spruce wood as affected by high-temperature drying. 2011. Wood and Fiber Science 43(2):206-214.
http://www.swst.org/wfs/journalOnline.html

Marc Borrega was responsible for planning and executing the experimental work, analyzing the results and writing the manuscripts for all papers. Petri P. Kärenlampi was involved in planning the experiments, discussing the results and commenting on successive versions of the manuscripts.

TABLE OF CONTENTS

1. INTRODUCTION

1.1. Wood composition

Wood is a natural polymeric material composed mainly of carbohydrates (cellulose and hemicelluloses) and lignin, with a minor portion of extractives. Cellulose, hemicelluloses and lignin are the structural components of the wood cell wall, whilst the extractives are low-molecular-mass compounds of different chemical nature, deposited primarily outside the cell wall (Sjöström 1981, Fengel and Wegener 1989). The chemical and structural composition of cellulose, hemicelluloses and lignin is briefly described in this section.

1.1.1. Cellulose

Cellulose is the most abundant component in wood, accounting for about 40 - 45 % of the dry wood mass in both softwoods and hardwoods. Cellulose is a linear polymer of β-D-glucopyranose units ($C_6H_{12}O_6$) linked together by β-(1-4)-glycosidic bonds (Sjöström 1981, Fengel and Wegener 1989). The actual repeating unit in cellulose is cellobiose, formed by two adjacent glucose monomers (Fig. 1). The degree of polymerization (DP) of cellulose in native wood is in the order of 10.000 glucose units, which corresponds to a molecular length of about 5 μm (Alén 2000).

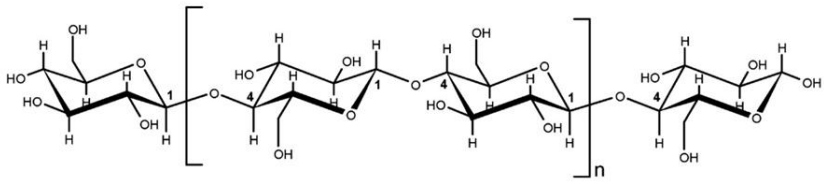

Figure 1. Structure of cellulose showing the repeating cellobiose unit.

Cellulose molecules aggregate into bundles called elementary fibrils, which in turn are aggregated into larger units called microfibrils (Sjöström 1981, Fengel and Wegener 1989). Elementary fibrils have a diameter ranging 2 - 4 nm, whereas microfibrils have a diameter ranging 10 - 30 nm (Fengel and Wegener 1989). These supramolecular structures are formed by hydrogen bonding between hydroxyl (-OH) groups in adjacent cellulose molecules (intermolecular linkage). There are also intramolecular linkages by hydrogen bonding between OH-groups in adjacent glucose units that belong to the same cellulose molecule. These intramolecular bonds are responsible for giving a certain degree of stiffness to the cellulose molecular chains (Fengel and Wegener 1989).

Cellulose microfibrils contain both crystalline and amorphous regions, depending on the degree of arrangement of the elementary fibrils. In crystalline regions, the fibrils are highly

ordered and regularly arranged, whereas in amorphous regions the fibrils have no definite arrangement. In Norway spruce, the crystallinity of cellulose has been reported to be 52 ± 3 % (Andersson et al. 2004). The orientation of the microfibrils within the cell wall, measured as the angular displacement from the fibre axis, has a major influence on the physical and mechanical properties of wood (Page et al. 1972, Cave 1976, Salmén and Burgert 2009).

1.1.2. Hemicelluloses

Hemicelluloses (polyoses) are amorphous and branched polymers composed of various sugar units. The main building units are pentoses such as xylose and arabinose, and hexoses such as glucose, mannose and galactose. Other less abundant sugar units belong to the groups of hexuronic acids and deoxyhexoses. The DP in hemicelluloses does not usually exceed 200 sugar units (Sjöström 1981, Alén 2000).

Hemicelluloses account for about 20 - 25 % and 25 - 30 % of the dry wood mass in softwoods and hardwoods, respectively. The chemical composition of hemicelluloses also differs between softwoods and hardwoods (Sjöström 1981, Fengel and Wegener 1989). In softwoods, the most abundant hemicellulose is galactoglucomannan (glucomannan), composed of galactose, glucose and mannose units. In hardwoods, the main hemicellulose is glucuronoxylan (xylan), composed of xylose units and 4-O-methylglucuronic acid groups (Fig. 2). Glucomannan in softwoods and xylan in hardwoods are partly substituted by acetyl groups (Sjöström 1981, Fengel and Wegener 1989).

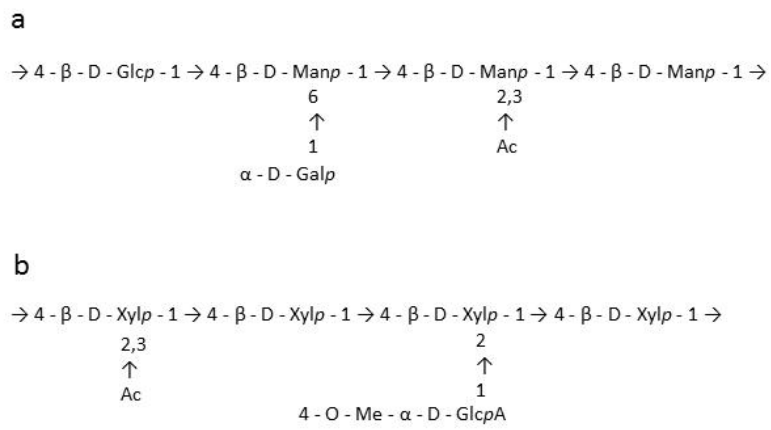

Figure 2. Abbreviated formulas for a) galactoglucomannan from softwood and b) glucuronoxylan from hardwoods. Sugar units: β-D-glucopyranose (Glc*p*); β-D-mannopyranose (Man*p*); β-D-galactopyranose (Gal*p*); β-D-xylopyranose (Xyl*p*); 4-O-methyl-α-D-glucopyranosyluronic acid (Glc*p*A). Ac is acetyl group (CH_3CO) (adapted from Sjöström 1981).

Hemicelluloses are believed to be closely associated to cellulose microfibrils, which in turn are embedded in a more or less random network of hemicelluloses and lignin (Timell 1967, Page 1976, Salmén 2004). Other authors suggest that hemicelluloses are regularly disposed between microfibrils, linking them together, with lignin filling some of the gaps (Vincent 1999, Yan and Zhu 2003). Hemicelluloses might also be present within amorphous regions of cellulose microfibrils (O'Sullivan 1997, Vincent 1999, Salmén 2004).

1.1.3. Lignin

Lignin, the third major component in wood, is an amorphous and high-molecular-mass polymer. Although composed of carbon, hydrogen and oxygen, lignin is not a carbohydrate but a complex polyphenolic compound built upon phenylpropane units (Sjöström 1981, Fengel and Wegener 1989). The building units do not follow any regular pattern of repetition, and it is not possible to isolate lignin from wood without inducing changes in its native state (Alén 2000). For those reasons, the chemistry and structure of lignin is not yet fully understood.

In general, lignin accounts for about 25 - 30 % and 20 - 25 % of the dry wood mass in softwoods and hardwoods, respectively. Lignin in softwoods is usually referred to as guaiacyl lignin, because more than 90 % of the building units are derived from trans-coniferyl alcohol, with the remainder being mostly derived from trans-p-coumaryl alcohol (Alén 2000). Lignin in hardwoods is referred to as guaicyl-syringyl lignin, because it contains about 50 % of trans-coniferyl and 50 % of trans-sinapyl alcohol-derived building units (Alén 2000) (Fig. 3).

The presence of lignin in wood gives rigidity to the cell wall. It also serves as a gluing agent by binding adjacent cells together. The term “lignin-carbohydrate complex” (LCC) is often used to describe the aggregate of lignin and carbohydrates by covalent bonding (Sjöström 1981, Fengel and Wegener 1989). However, despite the fact that chemical bonding has been reported between lignin and carbohydrates (Lawoko et al. 2004, Lawoko et al. 2005), the precise type and amount of bonds has not yet been clarified.

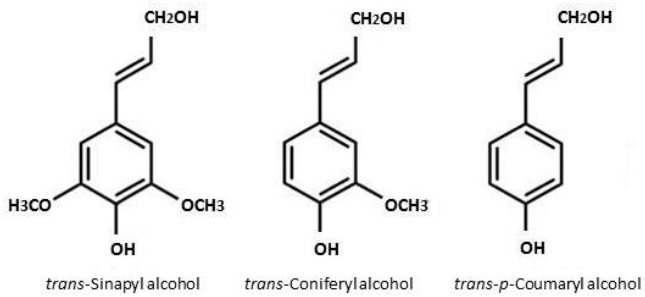

Figure 3. Main building units of lignin in wood.

1.2. Cell wall structure

Cellulose microfibrils, together with the surrounding network of hemicelluloses and lignin, are combined into lamellae to form the cell wall. The wood cell wall is primarily composed of two layers, the so-called primary (P) and secondary (S) walls. The secondary wall is, in turn, divided into three sub-layers that include the outer layer (S1), the middle layer (S2) and the inner layer (S3), each containing a different amount of lamellae. These layers also differ from one another in the orientation of the microfibrils and the relative distribution of wood components (Fengel and Wegener 1989, Haygreen and Bowyer 1996).

Wood fibres can be separated in earlywood and latewood fibres. Earlywood fibres are used by the living tree as transportation channels, whereas latewood fibres are used for mechanical support. For these reasons, latewood fibres have thicker cell walls and narrower lumen than earlywood fibres. The greatest difference between earlywood and latewood concerning cell wall thickness is found in the S2 layer. A schematic representation of the cell wall in both earlywood and latewood fibres is shown in Fig. 4.

The middle lamella (not shown in Fig. 4) is a thin layer primarily composed of lignin that binds adjacent cells together. The primary wall is the first layer deposited during the formation of the cell. It is a thin layer with cellulose microfibrils oriented more or less randomly (Brändström 2002). The transition between the middle lamella and the primary wall is not very clear, and thus the term “compound middle lamella” (CML) is often used to refer to the combination of middle lamella and adjacent primary walls (Fengel and Wegener 1989, Alén 2000). In spruce wood tracheids, the average thickness of the CML is about 0.09 µm (Fengel and Stoll 1973).

The secondary wall is a thick layer in which cellulose microfibrils have a very definite arrangement. In the S1 layer, the microfibrils are mostly oriented perpendicular to the fibre axis, with a microfibril angle (MFA) between 70 - 90 ° (Brändström 2002). However, lower MFA values, in the vicinity of 50 °, have also been reported (Paakkari and Serimaa 1984). In spruce wood tracheids, the average thickness of the S1 layer is about 0.26 and 0.38 µm for earlywood and latewood, respectively (Fengel and Stoll 1973).

The S2 layer of the secondary wall is, by far, the thickest layer in the cell wall. It also contains the highest amount of cellulose, as compared to any of the other layers. The microfibrils run almost parallel to the main fibre axis, with MFA values between 5 - 10 ° in latewood and 20 - 30 ° in earlywood (Paakkari and Serimaa 1984, Sahlberg et al. 1997, Brändström 2002). For many purposes, the S2 layer can be considered the most important layer within the cell wall because it largely determines the physical and mechanical properties of the fibre. In spruce wood tracheids, the average thickness of this layer is 1.66 and 3.69 µm for earlywood and latewood, respectively (Fengel and Stoll 1973).

The most inner layer, the S3 or tertiary (T) wall as sometimes denoted, is a thin layer composed of not more than six lamellae. There appears to be some disagreement regarding the orientation of microfibrils in the S3 layer. Paakkari and Serimaa (1984) have reported MFA values between 14 - 19 ° in Norway spruce, whereas other authors have reported much higher MFA values (Abe et al. 1992, Brändström 2002). In spruce wood tracheids, the thickness of the S3 layer is about 0.09 and 0.14 µm for earlywood and latewood, respectively (Fengel and Stoll 1973).

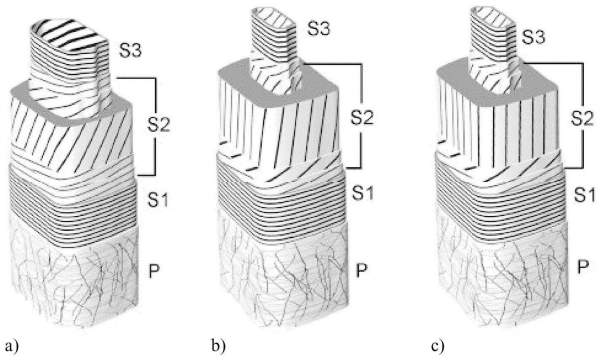

Figure 4. Example of a Norway spruce wood cell wall showing the orientation of cellulose microfibrils within and between different layers (P, S1, S2 and S3) for a) earlywood tracheid, b) latewood tracheid from juvenile wood, and c) latewood tracheid from mature wood (Brändström 2002).

1.3. Water in wood

Green wood contains a large amount of water, with moisture contents up to 200 %. Water in wood can be found in the lumens and within the cell walls. The disordered structure of the cell wall contains a vast number of pores of varying size and shape. The moisture content at which all liquid water has been removed from the lumen but the cell wall is still fully saturated is known as fibre saturation point (FSP). Water in the lumen exists as free liquid water and as water vapour. The term “free” is relative because liquid water is subjected to capillary forces and thus its thermodynamic properties are somewhat different than in the case of bulk water (Skaar 1988). Water within the cell wall, or bound water, is held tightly to adsorption sites by means of hydrogen bonding. The adsorption sites are mainly OH-groups in carbohydrates and lignin, although carboxylic acids may provide bonding sites as well (Berthold et al. 1994, Berthold et al. 1996). Hemicelluloses are often recognized as the most hydrophilic component in the wood cell wall, probably related to availability of free OH-groups. In the amorphous regions of the cellulose microfibrils, OH-groups are accessible to water adsorption. However, the crystalline regions are inaccessible to water molecules because all the OH-groups in adjacent cellulosic chains are expected to be mutually bound (Haygreen and Bowyer 1996).

In heterogeneous hydrated systems, the amount of water with depressed melting temperature is detectable by differential scanning calorimetry (DSC) (Rennie and Clifford 1977, Homshaw 1981, Ishikiriyama et al. 1995). The depressed melting temperature can be interpreted either as a consequence of some material constituents being partially solubilized or the material being microporous in such a way that surface tension of pure water depresses the melting temperature of water, because of small pore radius. The latter interpretation enables investigation of wood porosity in terms of thermoporosimetry (Maloney et al. 1998, Maloney and Paulapuro 1999, Maloney and Paulapuro 2001).

It is known that some water in hydrated porous systems does not freeze. This can be explained in a variety of ways. One of the simplest explanations is that in a space close in size to that of a molecule, there is not much room for molecular motion. Thus matter appears solid-like, regardless of temperature, and no thermal transition between solid and liquid is recognized (Berlin et al. 1970). Molecular mobility may also be reduced due to adsorption sites like ionic groups, ultimately forming a polymer gel (Berthold et al. 1994, Berthold et al. 1996). Alternatively, one might explain the existence of nonfreezing water (NFW) in terms of slowness of diffusion at low temperature and in small capillaries (Pouchlý et al. 1979, Kärenlampi et al. 2005). On this basis, water in the saturated porous cell wall can be divided into free water, freezing bound water and NFW (Nakamura et al. 1981). Free water is located in large pores and cavities, and has similar thermodynamic properties as pure bulk water. Thermal transitions of cell wall water differ between earlywood and latewood (Tynjälä and Kärenlampi 2001, Kärenlampi et al. 2005).

1.4. Heat treatments and thermal degradation of wood

In the last decade, an increasing interest in developing environmentally friendly methods for modifying wood properties has led to the production and commercialization of heat-treated wood. The exposure of wood to elevated temperatures during a heat treatment induces thermal degradation of the wood chemical structure, often accompanied by a loss of mass. As a result of thermal degradation, the physical and mechanical properties of wood are somewhat modified. Owing to the chemical changes in the wood structure and the modification of wood properties, thermal treatments are sometimes denoted as thermal modification processes. Several reports dealing with the properties of heat-treated wood have been published (Stamm et al. 1946, Tjeerdsma et al. 1998, Militz 2002, Bekhta and Niemz 2003, Esteves and Pereira 2009).

At temperatures above 100 °C, chemical bonds in wood begin to cleave. Between 100 ºC and 200 ºC, noncombustible products such as carbon dioxide, traces of organic compounds and water vapour are released (LeVan 1989, White and Dietenberger 2001, Hill 2006). Above 200 °C, significant thermal degradation of wood takes place, with major mass losses occurring beyond 250 °C. Cellulose, hemicelluloses and lignin degrade extensively in the temperature range between 300 - 400 ºC, 250 - 350 ºC, and 250 - 450 ºC, respectively (Beall and Eickner 1970, Bourgois and Guyonnet 1988, Alén et al. 1995, Kim et al. 2001, Hill 2006). Hemicelluloses are the least thermally stable polymers of the wood structural components (Bourgois and Guyonnet 1988, Zaman et al. 2000, Alén et al. 2002). The thermal stability of hemicelluloses is lower than that of cellulose, presumably due to their lack of crystallinity, a branched structure, and a lower degree of polymerization (Alén et al. 1996, Garrote et al. 1999). It is also evident that lignin, owing to its structural diversity, degrades gradually over a wider range of temperatures than carbohydrates. According to Stamm (1956), hemicelluloses degrade four times faster than wood, cellulose degrades at about the same rate as wood, and lignin degrades at about half the rate of wood. It has also been reported that, during pyrolysis, wood components degrade slightly more slowly as such than in their native state in wood (Alén et al. 1996).

The extent of thermal degradation is much dependent on the wood species and on the heat treatment conditions. Since hardwoods contain a higher proportion of hemicelluloses than softwoods, they are degraded more extensively when subjected to elevated temperatures (Zaman et al. 2000, Kamdem et al. 2002, Esteves et al. 2007). Mass loss increases with increasing treatment temperature and exposure time (Mitchell 1988, Hill 2006, Kocaefe et al. 2007, Esteves and Pereira 2009). The presence of air (oxygen), acids, and water in the heating atmosphere also affect the thermal degradation of wood. In the presence of air, the degradation of wood components is greater than in an inert atmosphere because of oxidation reactions (Stamm 1956, Mitchell 1988, Hill 2006). Organic acids, mainly acetic acid, released during the heating of wood catalyze the hydrolysis of wood components, in particular carbohydrates (Garrote et al. 1999, Hirosawa et al. 2001, Sundqvist 2004, Tjeerdsma and Militz 2005). In a closed system, where the acids formed cannot escape, the degradation of wood is more extensive than in a vented system (Stamm 1956, Mitchell 1988).

Thermal degradation in dry wood appears to be significant only above 200 ºC, though this temperature level dramatically decreases when wood is heated in moist conditions (Fengel and Wegener 1989, Passard and Perré 2004). Furthermore, the degradation of wood is much faster in the presence of moisture (steam or liquid water) than in a dry climate (Stamm 1956, Mitchell 1988). This is because in hydrothermal processes, hydronium ions generated through water autoionization accelerate the cleavage of acetyl groups linked to the hemicelluloses, with the consequent formation of acetic acid (Garrote et al. 1999, Garrote et al. 2001, Sundqvist 2004, Tjeerdsma and Militz 2005). It has been suggested that water needed for the hydrolysis of wood components is mainly provided by the moisture content of the wood, rather than any moisture available in the atmosphere (Källander and Bengtsson 2004).

Mass loss in heat-treated wood is largely due to degradation of the hemicelluloses, because their thermal stability is lower than that of cellulose and lignin (Bourgois and Guyonnet 1988, Zaman et al. 2000, Alén et al. 2002). The degradation of hemicelluloses comprises deacetylation and depolymerization reactions to form oligo- and monosaccharides (Garrote et al. 1999, Garrote et al. 2001, Sundqvist 2004, Tjeerdsma and Militz 2005). The monosaccharides may then be dehydrated into degradation products such as furfural or 5-hydroxymethylfurfural, depending on whether the sugar unit is a pentose or a hexose, respectively (Tjeerdsma et al. 1998, Weiland and Guyonnet 2003). Cellulose crystals are hardly degraded by thermal treatments at temperatures below 300 °C (Kim et al. 2001). However, degradation of amorphous cellulose, resulting in an increase in observed cellulose crystallinity, has been reported to occur during heat treatment of wood (Bhuiyan et al. 2000, Sivonen et al. 2002, Wikberg and Liisa Maunu 2004, Bhuiyan and Hirai 2005). Such changes in crystallinity appear to be more pronounced when wood is heated in moist conditions (Bhuiyan et al. 2000, Bhuiyan and Hirai 2005). In addition to chemical and structural changes in the carbohydrate components, thermal treatments induce cross-linking reactions within the lignin complex (Tjeerdsma et al. 1998, Sivonen et al. 2002, Weiland and Guyonnet 2003, Nuopponen et al. 2004, Wikberg and Liisa Maunu 2004).

As mentioned above, thermal degradation during a heat treatment results in wood products with modified properties. The main advantages of heat-treated wood are a reduction in hygroscopicity and an improved dimensional stability, generally believed to be due to the degradation of hygroscopic hemicelluloses (Hillis 1984, Feist and Sell 1987). Cross-linking reactions in the lignin complex, with a consequent reduction of available OH-groups, are also suggested to play a role on the reduced hygroscopicity and improved dimensional stability of heat-treated wood (Tjeerdsma et al. 1998, Weiland and Guyonnet 2003, Repellin and Guyonnet 2005, Tjeerdsma and Militz 2005). Additionally, the resistance of wood to biological attack appears to be improved after a heat treatment (Kamdem et al. 2002, Boonstra et al. 2006, Borrega et al. 2009). On a microstructural level, the removal of wood components due to thermal degradation is assumed to create cavities within the wood cell wall, as demonstrated by an increase in pore size (Hietala et al. 2002).

A decrease in mechanical properties, together with an increased brittleness, is the main drawback of heat-treated wood (Kubojima et al. 2000, Poncsák et al. 2006, Esteves et al. 2007, Kocaefe et al. 2007, Korkut et al. 2008), limiting its use to applications where good mechanical properties are not required. The poor mechanical performance is largely caused by the degradation of wood components, and particularly the degradation of the hemicelluloses (Winandy and Lebow 2001, Esteves et al. 2007).

Mechanical properties of heat-treated wood, although not explicitly specified, appear to have been generally tested at constant ambient conditions. The mechanical behaviour of wood is strongly dependent on its moisture content below the FSP (Gerhards 1982, Haygreen and Bowyer 1996). Since heat-treated wood is less hygroscopic than untreated wood, its mechanical properties under service conditions are likely to be higher than at constant moisture content.

1.5. Wood drying

Many applications of wood require that the material is dried from the green state to a pre-determined level between the FSP and the dry state. The principal reason for drying wood is to enhance its properties and thus increase its quality. As compared to thermal treatments, which aim to modify wood properties by inducing thermal degradation of the wood structure, wood drying processes aim to enhance wood properties by removing the water contained in the cell wall. Most physical properties of wood are not affected by changes in moisture content above the FSP. However, as soon as bound water is removed from the cell wall, the wood begins to shrink and its properties are modified. Dry wood has several advantages over green wood (Denig et al. 2000), such as: a) considerably lower weight, with reduced transport and handling costs, b) improved mechanical properties, in particular strength and stiffness c) lower risk of fungal attack, d) superior performance of fasteners, including nails and screws, and e) improved gluing, machining and finishing operations.

Wood drying may be regarded as a complex mass transfer process involving the movement of liquid water, molecular diffusion of bound water within the cell walls and water vapour within the lumens, and evaporation from the wood surface (Skaar 1988). Above the FSP, drying of wood is due to surface evaporation and movement of free liquid

water by capillary forces. Liquid water in the cell lumens is removed first because it is held less strongly than bound water. Below the FSP, drying of wood is due to molecular diffusion. Diffusion occurs as water molecules move from an area of high concentration to an area of lower concentration. This implies the existence of a moisture gradient or a water vapour pressure gradient across the wood cell wall as a driving force. The rate of diffusion is determined by the temperature, the severity of the moisture gradient and the microstructure of the material (Haygreen and Bowyer 1996).

Commercial wood drying is conducted in industrial kilns. Conventional kilns operate at temperatures up to 100 °C, while high-temperature kilns operate at temperatures above 100 °C. The latter are mainly used to dry softwood lumber. High-temperature drying can considerably reduce drying times as compared to conventional drying, thus reducing production costs. However, the quality of the dried wood material must be maintained if production costs are not to be offset by quality costs. Drying is the most expensive part of the primary wood chain and thus a lot of effort must be put in to avoid or minimize drying defects. Some defects are often due to a poor control of drying conditions, whilst others relate to the presence of natural defects in wood such as knots, spiral grain, tension/compression wood, *etc*. There are many types of drying defects, although they can basically be classified as checks and cracks, distortions (warp) and discoloration (Denig et al. 2000).

1.5.1. Hornification

As water in wood exits the pores during drying, the pores start to collapse, ultimately evolving into pore closure by irreversible hydrogen bonding between adjacent pore walls. Pore closure by irreversible hydrogen bonding in cellulose-rich pulps is a well-known phenomenon commonly denoted as hornification (Matsuda et al. 1994, Weise et al. 1996, Kato and Cameron 1999, Park et al. 2006). The occurrence of hornification results in a tightly bound structure, in which some of the polar sites previously available for water sorption do not open upon rewetting (Scallan 1977, Crawshaw and Cameron 2000). Therefore, irreversible hydrogen bonding decreases the capability of water sorption (hygroscopicity) in wood fibres. It has been suggested that hornification is due to covalent cross-linking within the lignocellulosic structure during drying (Fernandes Diniz et al. 2004), though to date no direct evidence of covalent bonding has been found, and thus hydrogen bonding between carbohydrate elements is generally accepted to be the leading mechanism behind hornification.

The main variable promoting hornification is the change in moisture content below the FSP along with drying. Hornification has been reported to occur at temperatures as low as 20 °C (Matsuda et al. 1994). Nonetheless, the degree of hornification also depends on the severity of the drying process, and in particular the drying temperature and the final degree of dryness (Matsuda et al. 1994, Weise 1998). Increased temperature increases the mobility of amorphous polymers in wood, thus inducing structural rearrangements and the consequent formation of irreversible hydrogen bonds. Increasing final dryness naturally increases the extent of pore closure. Hornification also appears to be enhanced with additional drying cycles (Weise 1998, Crawshaw and Cameron 2000). The occurrence of

hornification has usually been discussed in relation to pulp fibres rather than in relation to solid wood. Recently, however, it has been suggested that irreversible hydrogen bonding occurs in wood during drying, similar to that in pulp fibres, though to a lesser extent (Suchy et al. 2010a, Suchy et al. 2010b). The presence of the ligno-hemicellulosic matrix in wood may restrict the formation of hydrogen bonds within the fibres (Duchesne et al. 2001). In addition to hydrogen bonding, cross-linking in the lignin complex might also occur due to application of heat during drying (Tjeerdsma et al. 1998, Sivonen et al. 2002, Weiland and Guyonnet 2003, Nuopponen et al. 2004, Wikberg and Liisa Maunu 2004).

Structural changes within the wood cell wall due to hornification are expected to modify wood properties. As already mentioned, irreversible closure of pores is known to decrease the hygroscopicity of wood fibres (Scallan 1977, Matsuda et al. 1994, Weise et al. 1996, Kato and Cameron 1999, Crawshaw and Cameron 2000). Increased internal bonding between structural elements also renders the fibres stiffer and more brittle (Young 1994, Kato and Cameron 1999). Nonetheless, information regarding the occurrence of hornification and its effects on the physical and mechanical properties of solid wood in the scientific literature appears to be limited.

1.5.2. Microscopic cell wall damage

Microscopic cell wall damage occurs in wood during the course of drying (Kifetew et al. 1998, Thuvander and Berglund 1998, Thuvander et al. 2001). This damage is not due to the presence of moisture gradients within the wood, but is believed to be due to anisotropic drying shrinkage of cell wall layers, inducing internal stresses sufficient to damage the cell walls (Van den Akker 1961, Thuvander et al. 2002). The impregnation of wood with a chemical that reduces drying shrinkage may more than double the tensile strength of dried wood (Figure 5). Microscopic drying damage is manifested as microcracks irregularly distributed within the wood cell wall (Wallström and Lindberg 1999, Wallström and Lindberg 2000). Moreover, the NFW content in earlywood significantly increases after drying (Kärenlampi et al. 2005), most likely related to the microscopic drying damage.

Impregnation of wood with chemicals may not be the only way to reduce cell wall damage during drying. Wood is mostly composed of amorphous polymers and thus it shows time-dependent mechanical behaviour. Along with time, stresses within wood elements become reduced by stress relaxation, as a result of molecular reorganization. The molecular mobility of the amorphous polymers is dependent on the moisture content and on the temperature (Williams et al. 1955, Back and Salmén 1982, Kelley et al. 1987). The softening point at which amorphous polymers change from a glassy to a rubbery state is known as the glass transition temperature. It is generally recognized that, at high moisture contents, the relaxation behaviour in wood along with increasing temperature up to 200 °C is largely due to the softening of the lignin matrix (Cousins 1978, Salmén 1984, Irvine 1985). From the viewpoint of molecular reorganization, an increase in moisture content or temperature is analogous to an increase in available time. Therefore, relaxation of internal stresses that are responsible for creating the cell wall damage during wood drying may be favoured by conducting drying processes at elevated temperatures and with extended drying times.

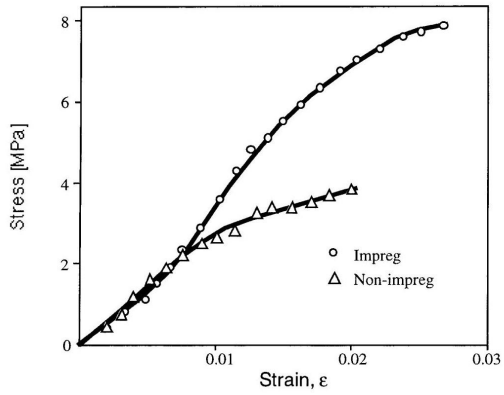

Figure 5. Stress-strain curve for dried microtomed earlywood specimens with and without chemical impregnation to avoid drying shrinkage. Impregnation was achieved by soaking wood specimens in a solution of water and glycerol (Thuvander et al. 2001).

1.6. Aims of the study

Wood is a natural material widely used in applications where a good mechanical performance is required. Before being placed under service conditions, wood is often dried to some extent below the FSP. During drying, microscopic cell wall damage occurs within the wood structure. Such damage is caused by large internal stresses arising from anisotropic drying shrinkage of cell wall layers. Microscopic cell wall damage remarkably reduces the load-bearing capabilities of the wood material. Drying damage may be minimized by conducting slow high-temperature drying processes, owing to the phenomenon of stress relaxation, and thus the mechanical behaviour of the dried wood might be improved.

Formation of irreversible hydrogen bonds (hornification) within the cell wall along with drying is a well-known mechanism. As a result of this increased internal bonding, the hygroscopicity of wood fibres is decreased, whereas the stiffness and the strength appear to be enhanced. Reduced hygroscopicity due to hornification may further improve the mechanical properties of wood under service conditions. Hornification is likely to be enhanced by high-temperature drying, owing to increased severity of the drying process.

Exposure of wood to elevated temperatures during high-temperature drying may induce thermal degradation of wood components. The mass loss that often accompanies the thermal degradation negatively affects the mechanical behaviour of wood. Temperature levels for thermal degradation appear to be lowered when wood is heated in moist conditions, as in drying of green wood.

The objective of this study was to investigate the mechanisms that occur during high-temperature drying of wood, and to evaluate their effects on the structure and properties of the dried products. Understanding the effects of such mechanisms may provide a good basis

for developing drying methods that improve the mechanical properties of dried wood. The particular aims of this study were:

- To investigate the effects of moisture and temperature with regard to thermal degradation of wood (Paper I).
- To investigate the effects of thermal degradation on the hygroscopicity and on the mechanical behaviour of wood at both constant moisture content and ambient conditions (Papers II-III).
- To evaluate the mechanical properties of high-temperature dried wood products in longitudinal and radial loading (Papers IV-V).
- To investigate the effects of high-temperature drying on cell wall porosity of earlywood and latewood fibres (Paper VI).

2. MATERIALS AND METHODS

2.1. Wood material

The wood material originated from Norway spruce (*Picea abies*) felled in Joensuu, Eastern Finland, during the autumn of 2005 (Papers I-IV) and 2008 (Papers V-VI). A tree was felled and its trunk was divided into two-metre long logs, with diameters comprised predominantly between 25 and 15 cm. The first 1.5 metres from the stump were discarded to avoid a significant presence of juvenile wood. The logs were immediately taken to a sawmill and cut into 32-mm (Papers I-IV) and 25-mm (Papers V-VI) thick boards. The boards were then stored in a freezer at -17 °C until preparation of specimens. Wood specimens with dimensions (longitudinal, radial, tangential) 320 x 24 x 24 mm^3 (Papers I-III), 350 x 20 x 20 mm^3 (Paper IV) and 55 x 100 x 20 mm^3 (Papers V-VI) were prepared. All specimens were clear of visible defects. Groups containing between 8 and 14 specimens each were prepared, and each group was subjected to a heat-bath treatment (Papers I-III) or to a high-temperature drying experiment (Papers IV-VI).

2.2. Heat-bath treatments

Heat-bath treatments were conducted in a stainless steel pressure vessel of 20 L volume, equipped with a temperature gauge, a pressure gauge and computer control. To block direct radiation from the steel onto the wood specimens, a sheet of aluminium was positioned at the bottom and around the walls of the vessel, as the radiant heat absorptivity and emissivity of aluminium are lower than those of stainless steel.

Before any heat-bath treatment, the wood specimens were oven-dried at 85 °C for 48 hours and their mass was measured. Dry masses were further determined by oven-drying an additional group of 24 reference specimens at 85 °C for 48 hours, and subsequently at 103

°C for 24 hours. Each group of specimens was then placed in the vessel along with a measured amount of liquid water, corresponding to a predetermined relative humidity at the setup temperature. The vessel was sealed and the temperature was raised. The heating rate was governed by the relative humidity in the vessel's atmosphere, the heating efficiency being limited by the heat transfer efficiency of the system. The presence of moisture may also affect the relaxation of stresses within wood specimens, although this effect may be partly balanced out by a decrease in available time. Water vapour pressure and consequent relative humidity in the vessel were determined by subtracting air pressure from the total pressure. Once the setup temperature was reached, the specimens were subjected to isothermal treatment, at the end of which the vessel was allowed to cool down slowly.

Table 1. Experimental parameters for the heat-bath treatments (Papers I-III). Standard deviation in parentheses.

Setup temperature (°C)	Liquid water added to the vessel[a] (g)	Relative humidity[b] (%)	Isothermal treatment (h)	Mass loss (%)	EMC (%)
120	-	15	0	-	10.1 (0.2)
	-	9	2	-	10.2 (0.2)
	-	5	8	-	10.0 (0.3)
	1000	100	0	-	9.9 (0.1)
	1000	100	2	-	9.7 (0.2)
	1000	100	8	-	9.1 (0.2)
150	-	8	0	-	9.3 (0.3)
	-	8	2	0.2 (0.3)	9.0 (0.3)
	-	8	8	0.4 (0.3)	8.7 (0.3)
	75	60	0	0.6 (0.2)	7.8 (0.2)
	75	51	2	1.0 (0.2)	7.3 (0.2)
	75	57	8	2.1 (0.3)	6.4 (0.2)
	1000	100	0	1.8 (0.5)	8.1 (0.1)
	1000	100	2	3.0 (0.7)	7.6 (0.1)
	1000	100	8	6.9 (1.3)	6.9 (0.2)
170	-	10	0	1.5 (0.5)	8.2 (0.2)
	-	15	2	2.1 (0.7)	7.8 (0.3)
	-	15	8	2.8 (0.9)	7.3 (0.3)
	65	55	0	2.4 (0.4)	6.5 (0.2)
	65	50	2	3.2 (0.5)	6.2 (0.2)
	65	61	8	7.2 (0.5)	5.6 (0.1)
	1000	100	0	6.2 (0.9)	7.2 (0.1)
	1000	100	2	10.9 (1.0)	6.6 (0.1)
	1000	100	6	15.3 (0.8)	6.2 (0.1)

[a] An additional amount of about 8 g of water was contained within any group of specimens
[b] Relative humidity at the instant of reaching the setup temperature

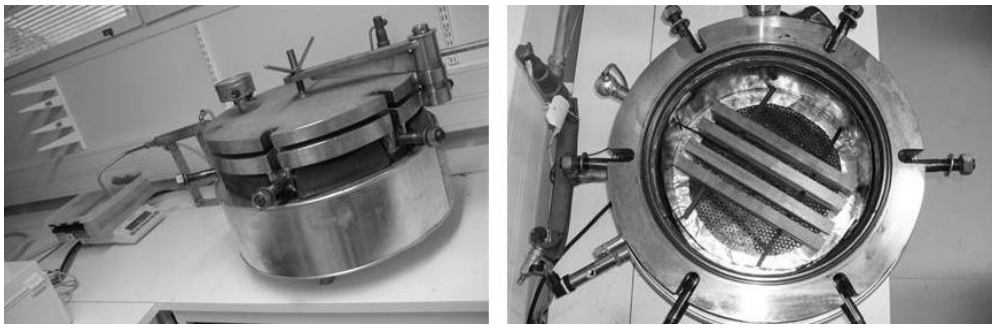

Figure 6. Pressure vessel used for the heat treatments and the high-temperature drying experiments. The moisture removed during the drying experiments was condensed in a container placed on a precision weight scale.

Heat-treated specimens were oven-dried at 85 °C for 48 hours and subsequently at 103 °C for 24 hours. Mass loss of any specimen was determined on a dry mass basis after oven-drying at 103 °C for 24 hours. The oven-dried specimens were transferred to a climate controlled room at 19 °C and 65 % relative humidity to attain equilibrium moisture content (EMC). Subsequently, a few specimens from each heat-treated group were placed in a climate controlled chamber at 19 °C, and the air humidity in the chamber was gradually increased until the specimens reached an EMC of 10.3 ± 0.1 %, which was the EMC at 19 °C and 65 % relative humidity of the oven-dried reference specimens. The experimental parameters for the heat-bath treatments are shown in Table 1.

2.3. Drying experiments

High-temperature drying experiments were conducted in the pressure vessel used for the heat-bath treatments, with the prior installation of a pressure valve to allow the removal of water vapour from the vessel. The removed water vapour was condensed in a container placed on a precision weight scale, which allowed monitoring changes in the wood moisture content throughout the whole drying process (Fig. 6).

Before any drying experiment, the initial moisture content of the wood was approximated by oven-drying either 30 mm end-pieces from the wood specimens (Paper IV) or 6 additional wood specimens (Papers V-VI) at 103 °C for 24 hours. Each group of specimens was then weighed and placed in the vessel. A measured amount of liquid water was added to the vessel to create a saturated steam atmosphere. The specimens were steamed in order to remove the effects of eventual variations in moisture content during storage in the freezer. In addition, the saturated steam atmosphere improved the heating efficiency of the system. The temperature in the vessel was raised to 128 °C and then the pressure valve was opened. Since the valve is in the upper part of the vessel, air exited first, with hot air over 125 °C being lighter than hot steam. After air removal, rapid water vapour removal followed until the moisture content of the wood was about 45 %. Thereafter, the

drying process was started at a predetermined temperature and drying rate. The drying rate was controlled by operating the pressure valve, the change in wood moisture content given by Eq. 1:

$$\frac{dM}{dt} = kM \tag{1}$$

where M (g/g) is the wood moisture content, t (s) is the drying time and k (s^{-1}) is the drying rate constant. After rearranging and integrating, Eq. 1 is transformed into:

$$\ln M = kt + C \tag{2}$$

where C is the integration constant. For $t = 0$, $C = ln\ M_0$, where M_0 is the moisture content at the beginning of the drying process (about 45 %). After substituting and rearranging, Eq. 2 can be rewritten as:

$$M_t = M_0 e^{kt} \tag{3}$$

where M_t is the moisture content of the wood at any time of the drying process.

Table 2. Experimental parameters for the drying processes (Paper IV). Standard deviation in parentheses.

Drying temperature (°C)	Drying rate[b] (-10^{-6} s^{-1})	Final moisture content (%)	Mass loss (%)	EMC (%)
80[a]	57.3	6.9 (1.9)	-	10.2 (0.6)
100[a]	93.7	5.8 (1.6)	0.2 (0.2)	9.6 (0.4)
110[a]	115.4	5.3 (0.8)	-	8.9 (0.2)
120[a]	205.7	5.3 (2.0)	-	9.0 (0.4)
130[a]	282.0	5.4 (1.9)	0.5 (0.5)	9.4 (0.5)
110	151.5	7.8 (2.7)	-	9.7 (0.7)
120	204.2	7.4 (2.3)	0.2 (0.5)	9.7 (0.6)
130	282.0	4.5 (1.5)	0.2 (0.7)	8.3 (0.4)
110	6.7	5.4 (1.0)	1.4 (0.9)	8.1 (0.3)
120	6.9	4.7 (0.9)	3.4 (0.8)	7.6 (0.4)
130	7.8	3.8 (0.3)	5.3 (0.4)	6.8 (0.2

[a] Drying processes conducted in a conventional laboratory oven

[b] Drying rates were computed according to Eq. 3 for the total drying time

Table 3. Experimental parameters for the drying processes (Papers V-VI). Data are shown as means with ± 95 % confidence intervals.

Drying temperature (°C)	Drying rate[a] (-10^{-6} s^{-1})	Final moisture content (%)	Mass loss (%)	EMC (%)
110	88.4	7.5 ± 2.3	0.2 ± 1.3	10.3 ± 0.6
120	105.0	7.4 ± 2.4	0.1 ± 2.3	10.3 ± 0.6
130	134.0	6.7 ± 3.0	0.5 ± 1.4	9.8 ± 0.6
110	6.8	5.1 ± 0.7	1.5 ± 1.5	8.7 ± 0.3
120	8.0	3.4 ± 0.4	2.2 ± 3.0	7.8 ± 0.2
130	6.9	5.5 ± 1.9	6.1 ± 1.2	7.9 ± 0.5

[a] Drying rates were computed according to Eq. 3 for the total drying time

In addition to the drying experiments in the pressure vessel, 5 groups of specimens were dried in a conventional laboratory oven at temperatures between 80°C and 130 °C (Paper IV). The corresponding drying rates were controlled by the atmospheric conditions in the oven. Before oven-drying, each group of specimens was steamed in the pressure vessel following the procedure described above. However, after reaching a moisture content of about 45 %, the vessel was cooled to about 100 °C and the specimens transferred to the oven. All dried specimens were placed in a climate controlled room at 19 °C and 65 % relative humidity to attain EMC. The mass loss of any specimen during drying was determined on a dry mass basis after oven-drying at 103 °C for 24 hours. The experimental parameters for the drying processes are shown in Table 2 (Paper IV) and Table 3 (Papers V-VI).

2.4. Mechanical properties

2.4.1. Bending tests

Mechanical properties of heat-treated wood and high-temperature dried wood (Papers III-IV) were determined in bending in an electromechanical testing device (Matertest 100 kN). Before the bending tests, heat-treated wood specimens were planed to cross sectional dimensions of 20 x 20 mm. Heat-treated wood was tested both at constant moisture content and at constant ambient humidity (Paper III). High-temperature dried wood specimens were tested at constant ambient conditions (Paper IV).

Bending experiments were conducted in a three-point bending apparatus with a span length of 300 mm (Fig. 7). The displacement of the cross-head was set to 0.2 mm per second, and the force was applied to the middle of the surface of the specimen nearest the pith. The modulus of rupture (MOR) and the modulus of elasticity (MOE) were determined according to:

$$MOR = \frac{3P_{\max}L}{2bh^2} \tag{4}$$

$$MOE = \frac{PL^3}{4bh^3\delta} \tag{5}$$

where P_{max} is the load at failure, P and δ are any load and its corresponding displacement below the proportional limit, L is the span length, and b and h are the width and the height of the specimen, respectively.

The strain at failure was determined according to equation 6:

$$\varepsilon_{\max} = \frac{6\delta_{\max}h}{L^2} \tag{6}$$

where ε_{max} and δ_{max} are the strain and displacement at failure, respectively. The failure strain was then divided into elastic failure strain (ε_e) and inelastic failure strain (ε_i). The elastic failure strain was computed as:

$$\varepsilon_e = \frac{MOR}{MOE} \tag{7}$$

and the inelastic failure strain was obtained by subtracting the elastic failure strain from the total failure strain.

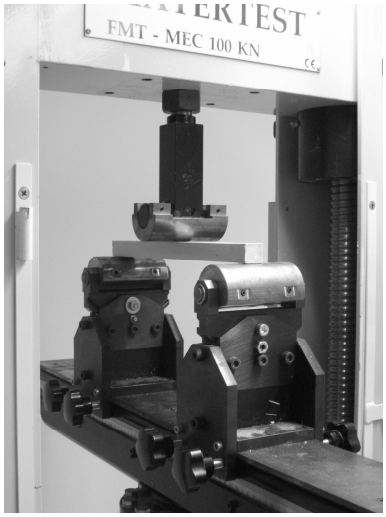

Figure 7. Three-point bending testing of heat-treated and high-temperature dried spruce wood.

The toughness of wood was determined as the area under the stress-strain curve up to failure, according to equation 8:

$$Toughness = \int_0^{\varepsilon_{\max}} \sigma d\varepsilon \tag{8}$$

where σ is the stress at strain ε. The toughness was divided into elastic and inelastic toughness. The elastic toughness was computed according to equation 9:

$$Elastic\ toughness = \frac{\varepsilon_e}{2} MOR \tag{9}$$

and the inelastic toughness was obtained by subtracting the elastic toughness from the total toughness.

2.4.2. Radial loading tests

In Paper V, the radial mechanical properties of high-temperature dried wood were determined in an electromechanical testing device (Matertest 100 kN) (Fig. 8), with the dried specimens machined to the required shape for mechanical testing in radial tension. The central section of the specimens was further reduced in the tangential direction by manual sanding. This was done to ensure that the specimens broke some distance away from the gripping edges. The displacement rate of the gripping claw was set to 0.02 mm per second, with both the force and the displacement recorded. The radial tensile strength was determined according to Equation 10:

$$\sigma_{\max} = \frac{F_{\max}}{A} \tag{10}$$

where σ_{max} (MPa) is the radial tensile strength, F_{max} (N) is the maximum force at failure and A (mm^2) is the cross-sectional area of the fractured specimen.

Due to the non-uniform cross sectional geometry of the specimens, the strain at a given stress could not be determined. However, an apparent strain at any stress was computed for each specimen as:

$$\varepsilon' = \frac{\Delta u}{l} \tag{11}$$

Figure 8. Mechanical testing of high-temperature dried wood in radial loading.

where ε' (mm/mm) is the apparent strain, Δu (mm) is the relative grip displacement, and l (mm) is the initial length of the specimen between the grips (45 mm). An apparent modulus of elasticity or apparent Young's modulus was subsequently computed as:

$$E' = \frac{\Delta\sigma}{\Delta\varepsilon'} \tag{12}$$

where E' (MPa) is the apparent Young's modulus, and $\Delta\sigma$ (MPa) and $\Delta\varepsilon'$ (mm/mm) are the incremental stress and its corresponding incremental apparent strain, respectively, determined between force of 30 N and 80 N.

2.5. Thermoporosimetry analyses

One specimen from each group subjected to high-temperature drying in Paper V was selected for thermoporosimetry analysis in Paper VI. An additional reference specimen was prepared from undried wood stored in a freezer for a few months. For any selected specimen, wood slices of 60 µm thickness were produced from both earlywood and latewood with a sliding microtome. At least 3 earlywood and latewood samples, containing 5 and 3 microtomed slices respectively, were prepared from each specimen. All samples were immersed in deionized water and kept in a refrigerator for a minimum period of 10 days prior to testing.

Before the thermoporosimetry analyses, each sample was chopped with a sharp knife and fitted in a sealed 40 µl aluminium pan. A small hole was then pierced to the pan to keep a constant pressure throughout the experiment. The pan was weighed and placed in a Mettler Toledo 823E differential scanning calorimeter. This device measures the amount of energy absorbed or released by a sample during a temperature change. The energy absorbed when the water in a frozen sample melts during a temperature increment is the sum of the

latent heat and the sensible heat. The latent heat is then used to determine the amount of water melted within the temperature step by means of the specific heat of melting. The experimental step program used for the thermoporosimetry analyses is shown in Table 4. An example of a heat flow during a DSC run is shown in Fig. 9. For every depressed melting temperature, a representative pore size (assuming a cylindrical pore shape) was computed through the Gibbs-Thomson equation:

$$D = \frac{-4 \cdot V_m \cdot \sigma_{ls}}{\overline{H}_m \cdot \ln \frac{T_m}{T_0}} \tag{13}$$

where D is the pore diameter (m), V_m is the molar volume of ice, σ_{ls} is the surface tension at the ice-water interface (20.4 mN/m (Ishikiriyama et al. 1995)), H_m is the specific heat of melting (334 J/g), T_0 is the melting temperature of bulk water (273.15 K) and T_m is the depressed melting temperature. The pore diameter corresponding to each depressed melting temperature is shown in Table 5.

Table 4. Experimental step program used in the thermoporosimetry analyses (Paper VI).

Step, n	Initial temperature (°C)	Heating ramp (°C/min)	Final temperature (°C)	Holding time at final temperature (min)
1	25	-10	20	6
2	20	-10	4	6
3	4	-5	-38	6
4	-38	1	-30	6
5	-30	1	-10	6
6	-10	1	-3	6
7	-3	1	-1	6
8	-1	1	-0.5	6
9	-0.5	1	-0.2	9
10	-0.2	1	-0.1	12
11	-0.1	-5	-38	6
12	-38	1	-36	6
13	-36	5	4	9
14	4	1	5	9
15	5	10	25	-

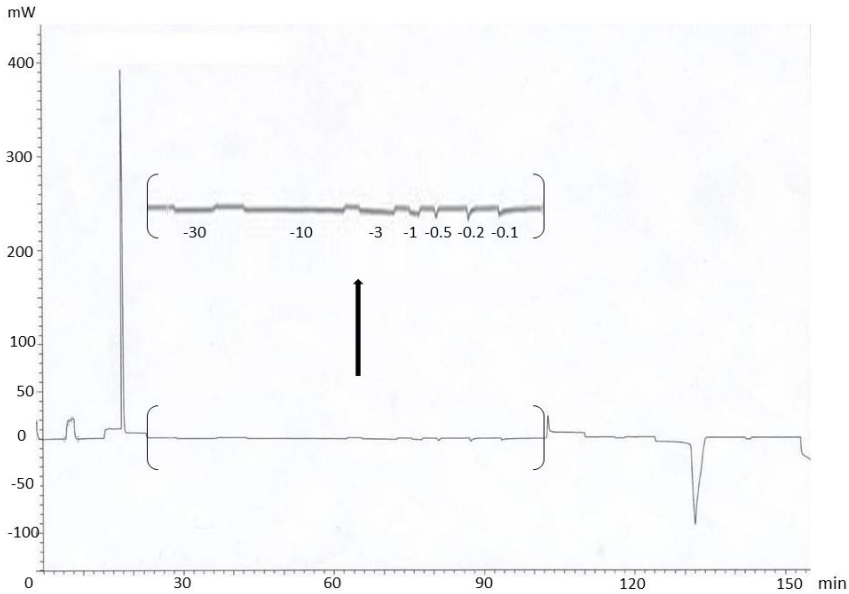

Figure 9. Example of heat flow during a DSC run, with a magnification of the isothermal step melting program (steps 4 to 10 in Table 4). The numbers in the magnified section are the depressed melting temperatures. The example corresponds to a latewood sample slowly dried at 120 °C.

Table 5. Pore diameter corresponding to the depressed melting temperature, computed by the Gibbs-Thomson equation (Eq. 13).

Melting temperature (°C)	Pore diameter (nm)
-38	1.8
-30	2.3
-10	7.2
-3	24.2
-1	72.7
-0.5	145.6
-0.2	364.1
-0.1	728.4

After the DSC experiment, each pan was weighed and subsequently oven-dried at 103°C for 24 h. The dry mass of any sample was 4.9 ± 0.2 mg, and its basic density ranged from 210 to 349 kg/m^3 for earlywood and from 509 to 826 kg/m^3 for latewood. The NFW content was quantified by subtracting the amount of freezing water to the total amount of water in the sample.

Because of the small hole pierced in the aluminium pan, some of the water in the sample evaporated during the DSC experiment. The total amount of water evaporated was

determined by weighing the pan immediately before and after the test. In addition, the amount of water evaporated was computed through the signal values (mW) given by the DSC instrument, the duration of any temperature step and the specific heat of vaporization (2260 J/g). A good agreement was found between measured and computed values for the evaporated water (Paper VI). Therefore, by using the signal values given by the DSC instrument, the actual amount of water within the pan at any instant of the experiment could be accurately determined.

The thermodynamic properties of water were determined by conducting six DSC runs with only deionized water. The experimental program applied was the same as shown in Table 4. All the energy absorbed by the water-only sample in the temperature interval from -38°C to -36°C and from 4°C to 5°C was considered to be a measure of its heat capacity. Average values for the specific heat capacity of ice (Cp_i) and liquid water (Cp_w) were 1.85 J/(g·°C) and 4.34 J/(g·°C), respectively. The specific heat of melting was computed to be 338.3 J/g.

2.5.1. Effect of phase change on the specific heat capacity

Detection of a first-order transition in terms of calorimetry requires detection of the latent heat related to that transition. This can be done by dividing the total applied/released heat into latent heat and sensible heat for the temperature change. The sensible heat related to temperature change can be computed provided the heat capacity of the specimen is known. Somewhat problematical is the fact that specific heat capacities change during phase transformations. The specific heat capacity of liquid water is more than two-fold that of ice.

In recent literature dealing with the application of calorimetry to wood and pulp fibres, latent heat has been determined by integrating over a base line characterizing the heat capacity of the specimen. The heat capacity, in turn, has been determined by linearly interpolating between temperatures well below and well above the range of melting temperatures (Maloney et al. 1998, Maloney and Paulapuro 2001, Kärenlampi et al. 2003a, Kärenlampi et al. 2003b, Kärenlampi et al. 2005). Linear interpolation of heat capacity over such a temperature range is generally incorrect. The result depends on the selection of temperatures between which the interpolation is done.

In Paper VI, a computational stepwise method that accounts for the change in specific heat capacity within any temperature step was developed. As in the case of water-only experiments, the heat capacity of any sample was determined by measuring the energy absorbed in the temperature range from -38°C to -36°C and from 4°C to 5°C. The heat capacity of the sample at temperatures below 0°C, however, could not be regarded as constant, but dependent on the amount of water melting in each temperature interval, given that the heat capacity of liquid water is higher than the heat capacity of ice. Furthermore, the heat capacity of ice is temperature-dependent, increasing about 10 % from -38°C to -10°C (Giauque and Stout 1936). Therefore, the heat capacity of any sample at a temperature step *n* below 0°C (see Table 4) was computed as:

for $n = 4$,

$$Cp_n = \left(Cp_0 + (W_n \cdot Cp_i) \cdot (1.05 - 1)\right) + Wm_n (Cp_w - 1.05 Cp_i) \quad (14)$$

for $n = 5$,

$$Cp_n = \left(Cp_{n-1} + (W_n \cdot Cp_i) \cdot (1.05^2 - 1.05)\right) + Wm_n (Cp_w - 1.05^2 Cp_i) \quad (15)$$

for $n = 6,\ldots 10$,

$$Cp_n = Cp_{n-1} + Wm_n (Cp_w - 1.05^2 Cp_i) \quad (16)$$

where Cp_n, W_n and Wm_n are the heat capacity of the sample, the mass of water in the sample and the mass of melted water in the temperature step n, respectively. Cp_0 is the heat capacity of the sample between -38°C and -36°C, and Cp_w and Cp_i are the measured heat capacity of liquid water and ice, respectively.

Eq. 16 was further used to compute the heat capacity of the sample between -0.1°C and 4°C, which was approximately equal to the heat capacity measured between 4°C and 5°C.

3. RESULTS

3.1. Effect of relative humidity on thermal degradation (Paper I)

The rate of temperature increment during the heat-bath treatments was governed by the relative humidity in the vessel's atmosphere, the heating efficiency being limited by the heat transfer efficiency of the system. Therefore, the extent of any heat-bath treatment, including heating, isothermal and cooling stages, was computed as:

$$H = \int_0^{t_f} (T(t) - T_0) dt \quad (17)$$

for $T(t) - T_0 \geq 0$, where H (°C·h) is the extent of heat-bath treatment, $T(t)$ (°C) the temperature in the vessel at time t, T_0 (°C) is a reference temperature and t_f (h) the duration of the process. The reference temperature was defined as the higher temperature at which mass loss does not occur, regardless of relative humidity conditions. A reference temperature of 120 °C was chosen on the basis of Table 1.

The rate of mass loss as a function of the extent of heat-bath treatment was evaluated as the first order reaction:

$$\frac{-dm}{dH} = Km \tag{18}$$

where m (g) was the mass of wood, H (°C·h) the extent of heat-bath treatment, and K $(°C·h)^{-1}$ the reaction rate constant. By integrating equation 18, it was possible to obtain:

$$\ln m = -KH + C \tag{19}$$

where C is the integration constant. In the case when $H = 0$, $C = \ln m_0$, with m_0 representing the initial mass of wood. Substituting and rearranging, equation 19 could be rewritten as:

$$\ln \frac{m_f}{m_0} = -KH \tag{20}$$

where m_f is the final mass of wood after the heat-bath treatment.

The rate of thermal degradation in wood was computed independently for every heat-bath treatment. Accordingly, the degradation rate increased with increasing temperature. Moreover, it increased, seemingly exponentially, with increasing relative humidity in the heating atmosphere. When compared to a dry climate (relative humidity range 5-15 %), thermal degradation at an intermediate relative humidity (50-61 %) was found to be three times faster at 170 °C, yet seven times faster at 150 °C. However, when compared to the intermediate relative humidity, thermal degradation in water-saturated conditions was about 4.5 times faster, irrespective of the setup temperature. This indicated that the increase in the degradation rate of wood along with increasing relative humidity from dry to water-saturated conditions cannot be a simple exponential function.

Temperature dependency of a reaction rate is often described in terms of activation energy, which can be computed by means of the Arrhenius equation. In the present case, the frequency factor of the equation had to be replaced by a constant with dimension inverse to the dimension of the extent of heat-bath treatment *H*. The modified Arrhenius equation was:

$$K = A\exp^{\frac{-E_a}{RT_S}} \tag{21}$$

where K (°C·h) $^{-1}$ is the reaction rate, A (°C·h)$^{-1}$ a pre-exponential factor replacing the frequency factor, E_a (kJ/mol) the apparent activation energy, R the universal gas constant (8.31 J/(mol·K) and T_S (K) the setup temperature. It is possible to rewrite Equation 21 as:

$$\ln K = \ln A - \frac{E_a}{R}\frac{1}{T_S} \tag{22}$$

Plotting ln K versus the reciprocal of the setup temperature for each relative humidity interval resulted in a straight line, with a slope denoted by E_a/R and an intercept ln A. This is often referred as an Arrhenius plot. As shown in Paper I, the apparent activation energy in a dry climate was the highest, which means that the temperature dependency of the degradation rate in dry conditions was higher than in moist conditions. Furthermore, heating of wood at intermediate relative humidity or in water-saturated conditions gave similar apparent activation energies. In other words, up to intermediate relative humidity, the drier the climate, the higher the temperature dependency of the degradation rate. However, at levels between intermediate relative humidity and water-saturated conditions, the temperature dependency appeared to be the same.

3.2. Hygroscopicity and mechanical properties of heat-treated wood (Papers II-III)

The EMC of oven-dried reference wood specimens under standard conditions (19 °C and 65 % relative humidity) was found to be 10.3 ± 0.1 %. Compared with the reference specimens, heat-treated wood clearly exhibited a reduction in hygroscopicity, its EMC ranging from 9.3 to 5.6 % (Paper II). It was found that the hygroscopicity of heat-treated wood decreased with increasing mass loss, regardless of the setup temperature and relative humidity condition. Furthermore, as a function of mass loss, data formed two different groups, specimens treated at intermediate relative humidity showing EMC levels some 2 % units lower than specimens treated either in dry or in water-saturated conditions. Therefore, hygroscopicity of heat-treated wood cannot be solely explained in terms of mass loss. Some other mechanism related to the relative humidity of the heating atmosphere appears to affect the hygroscopicity of wood.

The mechanical properties of heat-treated wood were tested in bending experiments (described in Paper III). At constant wood moisture content, the MOR of heat-treated wood was lower than that of the reference specimens, decreasing with increasing mass loss. The MOE was hardly affected up to a mass loss of about 3 %, though thereafter it decreased. As a function of mass loss, no differences among heat-bath treatments were found regarding the MOR and the MOE. At constant ambient humidity, the MOR and the MOE of heat-treated wood were improved up to a mass loss of about 2-3 %. When considering results as a function of mass loss, wood heated at intermediate relative humidity was found to be the strongest.

The elastic failure strain of heat-treated wood was within the range of 0.7-1 times that of the reference specimens. At constant ambient humidity, the elastic failure strain appeared to be greater than at constant moisture content. No major differences were found among treatments regarding the elastic failure strain, whereas the inelastic failure strain was clearly lower for wood heated in a dry climate. It was interesting to note that, at constant moisture content, wood heated at intermediate relative humidity showed higher inelastic ductility than that of the reference specimens. At constant ambient humidity, the inelastic ductility was reduced, being predominantly less than that of the reference specimens.

The elastic toughness of heat-treated wood was calculated according to Equation 9. At constant wood moisture content, the elastic toughness decreased with increasing mass loss, irrespective of the heat-bath process conditions. This result is a direct consequence of the MOR and the elastic failure strain decreasing with increasing mass loss, but no differences being found among the heat-bath treatments. At constant ambient humidity, the MOR as a function of mass loss was the highest for wood heated at intermediate relative humidity, whereas the elastic failure strain did not differ much among treatments. Consequently, as a function of mass loss, the elastic toughness was the highest for wood heated at intermediate relative humidity. At both constant wood moisture content and ambient humidity, the inelastic toughness was predominantly reduced by the heat-bath treatment. Moreover, as a function of mass loss, the inelastic toughness was the lowest for wood heated in a dry climate, which is in accordance with its lower inelastic ductility.

3.3. Mechanical properties of high-temperature dried wood (Papers IV-V)

3.3.1. Bending tests

The mechanical strength and stiffness of any porous material depends on its porosity. The density of the wood specimens used in Paper IV ranged from 325 to 460 kg/m^3, and thus the mechanical properties varied accordingly. Since our main interest was to investigate the effect of drying conditions on the mechanical properties of wood, the specific strength and specific stiffness, i.e., the MOR and the MOE divided by the density, were analyzed.

Specific MOR and MOE values decreased with increasing EMC. It was found that wood specimens that underwent slow drying attained the lowest EMC, and correspondingly, their specific strength and stiffness appeared to be the highest. The moisture content, however, only explained a small part of the variation in the specific MOR and MOE of dried specimens.

Surprisingly, the specific MOR remained unchanged in dried wood in cases where mass losses were up to 6 %, while the specific MOE seemed to increase slightly with increasing mass loss. This behaviour might be partly due to the correlation between the mass loss and the EMC, in particular for those specimens that were slowly dried (Table 2). Nonetheless, other mechanisms contributing to the strength and stiffness of dried wood may exist, beyond the reduced hygroscopicity. This is further supported by the fact that the specific MOR, and to a lesser extent the specific MOE, appeared to decrease along with increasing the final moisture content reached during drying.

Inelastic ductility of dried wood increased with increasing the EMC, but decreased with increasing the mass loss and the final dryness reached during drying. On the other hand, the drying process parameters had little effect on elastic ductility. Therefore, any variation in wood ductility due to drying conditions was governed by changes in inelastic ductility.

3.3.2. Radial loading tests

High-temperature dried wood specimens were found to show a characteristic force-elongation curve during radial loading (Paper V). Accordingly, wood specimens exhibited an initial elastic behaviour before the curve reached a plateau, and thereafter the force continued to increase until fracture occurred. After the plateau, the increase in force as a function of elongation was less pronounced than that exhibited during the elastic region. Only a few dried specimens broke before the force-elongation curve reached the plateau.

For both rapidly dried and slowly dried wood, the results of average radial tensile strength appeared to be the highest for specimens dried at 120 °C. Regardless of drying temperature, slow drying resulted in wood specimens with a somewhat lower radial tensile strength. Such effect may be due to the higher mass loss that occurred in processes with extended drying times (Table 3).

Wood specimens that were rapidly dried at 120 °C were not only the strongest, but also the most ductile, with most of these specimens showing ductility values well above 2 %. The rest of drying conditions resulted in wood specimens with similar apparent ductility. Specimens that were slowly dried at 130 °C appeared to have the lowest apparent stiffness. The values of apparent stiffness, however, may depend on the definition adopted in Equation 12 for the determination of the apparent Young's modulus.

The effect of drying parameters on the radial mechanical properties of wood was analyzed by plotting a table of linear correlation coefficients. The radial tensile strength was predominantly explained by the apparent ductility. Otherwise the mechanical properties of wood seemed to correlate poorly with any drying parameter. Nonetheless, it is interesting to note that the EMC was strongly explained by both the final moisture content reached during drying and by the drying rate. The mass loss, however, explained only a minor part of the EMC.

3.4. Cell wall porosity in wood as affected by high-temperature drying (Paper VI)

The amount of pore water in earlywood and latewood after high-temperature drying and rewetting was investigated by DSC. The pore size distribution in the wood cell wall was then related to the measured amount of pore water. According to the results from the DSC experiments, the NFW content in all samples was predominantly between 20-30 % of the dry wood mass. Similar amount of NFW was found in both earlywood and latewood, the average values being 0.23 g/g and 0.25 g/g, respectively.

Up to a pore size of 24 nm, the pore size distribution in earlywood and latewood appeared to be almost identical. However, earlywood contained more pores of larger size, with almost twice as much pore water as latewood in pores of 300-800 nm. It was

interesting to note that, for a few earlywood samples, the total amount of bound water well exceeded the dry mass of wood.

Earlywood sections in all dried specimens contained less bound water than native earlywood. Drying appeared to close cavities of the largest size (over 145 nm), whereas no clear effects on the smaller pores could be observed. Moreover, the amount of bound water in dried earlywood decreased with increasing drying temperature and drying time. Both earlywood and latewood sections from specimens slowly dried at 130 °C had the lowest amount of bound water, regardless of the pore size. Slow drying processes also appeared to result in lower NFW content in earlywood.

4. DISCUSSION

4.1. Thermal degradation and its effects on the properties of wood

Exposing wood to elevated temperatures can cause thermal degradation of its chemical structure, often resulting in a loss of mass. In this work, the mass loss in spruce wood during a heat-bath treatment increased with increasing temperature and exposure time beyond 120 °C (Paper I). Furthermore, the mass loss increased with increasing the relative humidity in the heating atmosphere. Previous studies dealing with heat treatments of wood have reported similar results regarding the effect of increasing temperature and time on the mass loss of wood (Mitchell 1988, Hill 2006, Kocaefe et al. 2007, Esteves and Pereira 2009). It has also been shown that heating wood in water-saturated conditions induced higher mass losses compared to heating in dry conditions (Stamm 1956, Mitchell 1988).

Wood exposed to temperatures between 100 °C and 200 °C produces water vapour and other noncombustible products like carbon dioxide and carboxylic acids, specifically acetic acid (LeVan 1989, White and Dietenberger 2001, Hill 2006). The acetic acid, formed through the cleavage of acetyl groups bound to the hemicelluloses, further catalyzes the degradation of carbohydrates (Garrote et al. 1999, Hirosawa et al. 2001, Sundqvist 2004, Tjeerdsma and Militz 2005). In the presence of water, the formation of acetic acid is accelerated because hydronium ions generated by water autoionization catalyze the splitting of the acetyl groups (Garrote et al. 1999, Garrote et al. 2001, Sundqvist 2004, Tjeerdsma and Militz 2005). Therefore, at any temperature, increasing the amount of water within the system by increasing the relative humidity in the heating atmosphere would be expected to induce higher mass losses in wood, as described in full in Paper I.

The mass loss after exposure to elevated temperatures could be mainly attributed to the degradation of hemicelluloses, known to be the least thermally stable polymers of the main wood components (Bourgois and Guyonnet 1988, Zaman et al. 2000, Alén et al. 2002). The poor thermal stability of hemicelluloses is presumably due to their low degree of polymerization, as well as to their branched and amorphous structure. Chemical reaction rates tend to increase as a function of increasing molecular mobility of the reactants. High temperatures soften the amorphous polymers in wood, so increasing their mobility

(Williams et al. 1955, Back and Salmén 1982, Kelley et al. 1987, Fahlén and Salmén 2003). The softening point at which amorphous polymers change from a glassy state to a gel-like state is known as the glass transition temperature. In a dry climate, the softening of the hemicelluloses takes place in the vicinity of 180 °C, but in the presence of moisture, the glass transition temperature is reduced (Back and Salmén 1982, Fengel and Wegener 1989, Åkerholm and Salmén 2004).

During a heat-bath treatment in dry conditions, the hemicelluloses in wood were rather stiff up to a temperature of 150 °C, but somewhat more viscous at 170 °C (Paper I). During a heat-bath at intermediate relative humidity (50-61 %), the hemicelluloses were probably viscous at both 150 °C and 170 °C. Therefore, increasing relative humidity at 150 °C was expected to have a greater effects on the thermal degradation of wood than at 170 °C, due to the change in state of the hemicelluloses. Increasing the relative humidity from intermediate conditions to water-saturated conditions increased the rate of degradation, but the effect would be the same at both temperatures since the hemicelluloses were already plasticized. This may partly explain the fact that, as compared to dry conditions, thermal degradation rates at intermediate relative humidity were 7 times faster at 150 °C but only 3 times faster at 170 °C (Paper I). It may also explain that, along with increasing relative humidity from intermediate to water-saturated conditions, the increase in the degradation rate was the same at both 150 °C and 170 °C.

The particular effect of heating in a moist climate on the degradation of wood was further supported by the temperature dependency of the thermal degradation rate. The temperature dependency of the degradation rate may be described by the activation energy. In Paper I, the apparent activation energy in dry conditions was found to be about three times higher than in moist conditions. Stamm (1956) reported that the activation energy in dry conditions was about two-times higher than in water-saturated conditions. On the other hand, the apparent activation energy of the degradation rate at intermediate relative humidity and water-saturated conditions was the same (Paper I). This is in agreement with the fact that increasing relative humidity, from intermediate to water-saturated conditions, had the same effect on the degradation rate regardless of the setup temperature.

An additional factor possibly affecting the increase in mass loss along with increasing relative humidity in the heating atmosphere is related to heat transfer phenomena. At any temperature, increasing relative humidity within the vessel results in increased wood moisture content. A greater presence of moisture may facilitate heat conduction from the surrounding ambient into the inner wood structure, thus enhancing the extent of thermal degradation.

The mass loss that accompanied thermal degradation affected the physical and mechanical properties of wood. In Paper II, the hygroscopicity of heat-treated wood was lower than that of reference wood specimens, decreasing with increasing mass loss. Hemicelluloses are regarded as one the most hygroscopic components within the wood cell wall (Hillis 1984, Feist and Sell 1987, Bekhta and Niemz 2003). Therefore, if hemicelluloses were degraded during a heat-bath treatment (Bourgois and Guyonnet 1988, Zaman et al. 2000, Alén et al. 2002), the capability of wood to adsorb moisture would be reduced. Additional reduction in hygroscopicity may be due to cross-linking reactions in

the lignin complex (Tjeerdsma et al. 1998, Sivonen et al. 2002, Weiland and Guyonnet 2003, Nuopponen et al. 2004, Wikberg and Liisa Maunu 2004).

The hemicelluloses, as one of the main wood structural components, play an important role in the mechanical behavior of wood (Winandy 2001, Winandy and Lebow 2001, Åkerholm and Salmén 2001, Bergander and Salmén 2002, Salmén 2004). At constant wood moisture content, the MOR of heat-treated wood was lower than that of untreated wood, decreasing with increasing mass loss (Paper III). In general, the MOE of heat-treated wood was unaffected up to a mass loss of about 3 %, but thereafter it decreased with increasing mass loss. These results were in agreement with previous studies indicating that stiffness is less sensitive to mass loss than strength (Bekhta and Niemz 2003, Poncsák et al. 2006, Esteves et al. 2007). Toughness and ductility of heat-treated wood were also reduced as compared to untreated wood, as already reported by Kubojima et al. (2000). Based on these results, mechanical properties of wood in bending were strongly influenced by the mass loss that occurred as a result of the degradation of hemicelluloses.

In addition to constant wood moisture content, the mechanical properties of heat-treated wood were tested at constant ambient conditions (Paper III). In these circumstances, and up to a mass loss of 2-3 %, the MOR and the MOE of heat-treated wood were higher than those of untreated wood. Decreasing moisture content in wood below the FSP is known to result in an improvement of mechanical properties (Gerhards 1982, Haygreen and Bowyer 1996). Therefore, the reduced hygroscopicity of heat-treated wood was likely to be responsible for the increase in MOR and MOE up to a mass loss of 2-3 %. Owing to the lower moisture content, the ductility of heat-treated wood at constant ambient conditions was decreased, which was in agreement with previous observations (Stone 1955, Reiterer and Tschegg 2002, Obataya et al. 2006).

As a function of mass loss, specimens that were heated at intermediate relative humidity showed an EMC about 2 % lower than specimens heated either in dry or in water-saturated conditions (Paper II). Furthermore, specimens heated at intermediate relative humidity exhibited the highest inelastic ductility when tested under constant ambient conditions, despite their EMC being the lowest (Paper III). This indicated that some mechanism occurring during a heat-bath treatment at intermediate relative humidity, as compared to dry or water-saturated conditions, must be involved in the reduced hygroscopicity and the increased inelastic ductility of heat-treated wood.

The effect of mass loss on the hygroscopicity and on the mechanical properties of wood was further investigated after high-temperature drying (Papers IV-V). Slowly dried wood experienced considerably higher mass loss than rapidly dried wood, and correspondingly, their hygroscopicity was the lowest (Tables 2 and 3). This was in agreement with the results reported in Paper II. However, regarding the mechanical properties in bending, the MOR and MOE of slowly dried wood were hardly affected by mass loss (Paper IV). In radial loading, the strength and stiffness of dried wood specimens with considerable mass loss were rather high (Paper V). The increased mechanical performance of slowly dried wood may be partly explained by the lower hygroscopicity (Gerhards 1982, Haygreen and Bowyer 1996). Nonetheless, it is unlikely that the mechanical properties of dried wood could be solely explained on the basis of the EMC or the mass loss (Papers IV-V). This was

further supported by the effect of the final moisture content reached during drying on both the hygroscopicity and the mechanical properties of wood.

4.2. Other mechanisms affecting the properties of heat-treated and high-temperature dried wood

The reduction in water-adsorption capability of pulp fibres along with drying is generally accepted to be due to irreversible hydrogen bonding between amorphous carbohydrates in the cell wall (Matsuda et al. 1994, Weise et al. 1996, Kato and Cameron 1999). As water exits the pores during drying, the pore walls start to collapse, eventually resulting in irreversible hydrogen bonding (Scallan 1977, Matsuda et al. 1994, Weise et al. 1996, Kato and Cameron 1999, Crawshaw and Cameron 2000, Park et al. 2006). The formation of irreversible hydrogen bonds during drying is often denoted as hornification. Additional drying cycles appear to enhance the occurrence of hornification (Weise 1998, Crawshaw and Cameron 2000).

In terms of the heat-bath treatments reported in Papers I-III, intermediate relative humidity at the setup temperature was produced by placing dry wood specimens in the pressure vessel, together with a predetermined amount of liquid water. Added water penetrated the wood specimens, entering more readily the large pores and cavities, but also eventually entering the smaller pores over a period of time. Further on, increased temperature in the vessel lowered the relative humidity in the heating atmosphere. Thus some of the water that had entered the wood vaporized, inducing a drying sequence in the disordered pore system of the cell walls. Naturally, high-temperature drying did not occur in specimens heated in water-saturated conditions; on the other hand, specimens heated in a dry atmosphere were not wetted during the experiment. Only those specimens treated at intermediate relative humidity experienced a wetting and high-temperature drying cycle, with the consequent formation of irreversible hydrogen bonds within the wood cell walls. Some of the hydrogen bonds formed may not be truly irreversible, as they partly appear to re-open when wood is exposed to high relative humidity (Obataya 2007). Nonetheless, this hornification may explain the lower hygroscopicity of specimens heated at intermediate relative humidity, as shown in Paper II.

The moisture sorption capability of wood after a heat-bath treatment may be affected not only quantitatively, but also qualitatively. Obataya (2007) showed that, as a function of mass loss, the EMC of dry-heated wood exposed to high relative humidity (97%) was considerably lower than that of steamed wood, due to a reduction in the amount of dissolved (multi-layered) water. Dry heating induced structural rearrangements in the wood polymeric chains, such as cross-linking and hydrogen bonding, which minimized the intermolecular spaces and consequently reduced the amount of dissolved water present in wood (Yasuda et al. 1994, Obataya 2007). Under water-saturated conditions, however, a tight structure could not be formed as the intermolecular spaces in wood were maximized by the adsorption of water. Structural rearrangements may be enhanced during a heat-bath treatment at intermediate relative humidity, because water acts as a plasticizer and provides further flexibility to the cell wall (Becker and Noack 1968). In the experiments reported by

Obataya (2007), the amount of hydrated (mono-layered) water, which mostly reflects the number of active adsorption sites in wood, decreased similarly in both dry-heated and steamed wood along with the degradation of hemicelluloses Exposure of wood heated under dry, moist and water-saturated conditions to cycles of low and high relative humidity may be needed to further elucidate the effects of relative humidity in the heating atmosphere on the quantitative and qualitative sorption of water.

The mechanical behaviour of wood is expected to be altered as a result of increased internal bonding within the fibre cell wall. Hornified fibres have been reported to be stiffer than undried fibres (Young 1994, Kato and Cameron 1999). Therefore, irreversible hydrogen bonding in wood specimens heated at intermediate relative humidity might account for their greater mechanical performance, including their inelastic ductility (Paper III). The formation of hydrogen bonds in the amorphous carbohydrates may be manifested as an increase in cellulose crystallinity, which could improve the mechanical properties of wood in the longitudinal direction. Furthermore, the crystallization of cellulose was probably promoted by the heat treatment, particularly in the presence of moisture (Bhuiyan et al. 2000). As thermal treatments appear to yield wood products with properties similar to those of naturally aged wood (Obataya 2007, Matsuo et al. 2011), the overall superior performance of wood heated at intermediate relative humidity could be important for developing processes such as the artificial ageing of wood.

In Papers IV-V, the EMC of dried wood was shown to decrease along with increasing final dryness. This was in agreement with previous studies reporting that the extent of hornification depends on the severity of the drying treatment (Matsuda et al. 1994, Weise 1998, Crawshaw and Cameron 2000). Furthermore, as a function of final dryness, slowly dried specimens clearly showed lower EMC than rapidly dried specimens. This could be partly explained by the higher mass loss that occurred in slowly dried specimens. Nonetheless, additional hornification may occur in drying treatments with extended drying times.

In order to better understand this, it is necessary to consider the case of a water droplet located in a small pore within the wood cell wall. During the drying process, the droplet will exit the pore, and the surface tension of the diminishing water droplet will bring the pore walls closer to each other, attempting to close the cavity. The pore closure, however, deforms the cell wall structure, thus inducing elastic stresses within the cell wall material which counteract the pore closure. Wood polymers show time-dependent mechanical behaviour, manifested either as creep or as stress relaxation (Bodig and Jayne 1993). Along with time, the elastic stresses in the cell wall relax, and the cell wall material creeps. Thus the pore closure is likely to be more complete in a slow drying process, in comparison with a rapid one, because it is aided by stress relaxation and creep. This is the reason why greater levels of hydrogen bonding between wood elements can be expected in slow drying processes.

The strength and the stiffness of high-temperature dried wood in longitudinal and radial loading were found to be hardly affected by large variations in mass loss (Papers IV-V). This was particularly true in the case of slowly dried wood, which not only experienced higher mass losses, but also a higher degree of hornification. It thus appears that, regarding the mechanical behaviour of wood, irreversible hydrogen bonding within the wood

structure competed with the effects of mass loss. Additionally, reduced EMC due to hornification may further increase the mechanical properties of dried wood. On the basis of the results in Papers IV-V, mechanical properties in radial loading were somewhat more sensitive to mass loss than in longitudinal loading.

Inelastic ductility of dried wood was negatively affected by the hornification and the mass loss in Paper IV. However, the occurrence of hornification has been suggested above as a possible explanation for the highest inelastic ductility of wood heated at intermediate relative humidity (Paper III). This apparent contradiction with the results in Paper IV could be due to different experimental arrangements. In Paper III, the wood specimens were subjected to a heat-bath which included wetting, high-temperature drying, and rewetting along with decreasing temperature. In Paper IV, high-temperature drying was not followed by rewetting, which might have recovered the inelastic ductility of the samples tested.

Significant microscopic damage occurs in the wood cell wall during drying. This damage is due to anisotropic drying shrinkage of cell wall elements, inducing internal stresses large enough to damage the wood cell wall (Van den Akker 1961, Thuvander et al. 2002). The microscopic damage strongly affects the mechanical properties of wood. The impregnation of wood with a chemical that reduces drying shrinkage appears to more than double the tensile strength of thin earlywood specimens (Thuvander et al. 2001).

Impregnation of wood with chemicals might not be the only way to reduce microscopic cell wall damage. Relaxation of internal stresses in wood during drying, and the consequent reduction of cell wall damage, may also be accomplished by conducting high-temperature drying processes with extended drying times. This is because stress relaxation within the wood amorphous polymers is favoured by increasing temperature, moisture content, and available time for molecular reorganization (Williams et al. 1955, Back and Salmén 1982, Kelley et al. 1987).

Slow high-temperature drying experiments were conducted in Papers IV-V. According to the results, the effects of microscopic cell wall damage on the mechanical properties of macroscopic wood specimens were not clearly identified. The incompatibility of drying shrinkage is pronounced when the microfibril angle varies within or between cell wall layers. In wood fibres, the S1 and S3 layers have large and widely varying microfibril angles, whereas in the S2 layer the microfibril angle is rather uniform (Paakkari and Serimaa 1984, Sahlberg et al. 1997, Brändström 2002). The drying damage is thus most pronounced in the S1 and S3 layers, as well as in tracheids with a small proportion of the S2 layer, *i.e.*, earlywood tracheids. In longitudinal tension, latewood fibres carry a significant portion of the total load. This is not only due to the greater density of latewood, but also because it contains a higher proportion of the S2 layer, with a relatively small microfibril angle (Paakkari and Serimaa 1984, Sahlberg et al. 1997, Brändström 2002). In the bending experiments reported in Paper IV, drying damage was most pronounced in those sections of the microscopic structure of wood which actually carried a relatively small part of the total load. Consequently, drying damage may drastically reduce the strength of thin earlywood specimens (Thuvander et al. 2001), but it hardly affected the strength of the entire wood structure loaded in the longitudinal direction (Paper IV).

In radial loading, the contribution of the S1 and S3 layers to the mechanical properties of wood is notable (Åkerholm and Salmén 2001, Bergander and Salmén 2002, Salmén

2004, Salmén and Burgert 2009). Therefore, the effects of drying damage might possibly be observed not only in microtomed sections, but also in macroscopic wood specimens loaded in the radial direction. According to Paper V, however, such effects could not be identified. The mechanical behaviour of wood loaded in different directions is largely determined by the structural composition of the cell wall. The hemicelluloses in the S1 and S3 layers have a strong influence on the radial mechanical properties of wood, whereas cellulose microfibrils mainly govern the mechanical properties in longitudinal loading (Åkerholm and Salmén 2001, Bergander and Salmén 2002, Salmén 2004, Salmén and Burgert 2009). In a slow high-temperature drying process, stress relaxation may indeed reduce the microscopic cell wall damage, but hemicelluloses in wood will also degrade, thus reducing the radial mechanical behaviour of wood. As shown in Paper V, the degradation of wood components, mainly hemicelluloses, during a slow high-temperature drying process appeared to counter any benefit achieved by stress relaxation.

4.3. Effects of high-temperature drying on the porosity of the wood cell wall

As discussed above, three mechanisms that occur during high-temperature drying, *i.e.*, thermal degradation, hornification and microscopic cell wall damage, affect the physical and mechanical properties of wood. These three mechanisms may also affect its porosity. In the first case, thermal degradation of wood components after exposure to elevated temperatures (Stamm 1956, Hill 2006, Esteves and Pereira 2009) may result in the formation of cavities within the cell wall. It has been shown that the removal of hemicelluloses and lignin during pulping created new pores within the fibre cell wall (Stone and Scallan 1967, Maloney and Paulapuro 1999). In the second case, as water exits the pores during drying, the pore walls start to collapse, eventually evolving into pore closure by irreversible hydrogen bonding, *i.e.*, hornification (Scallan 1977, Weise et al. 1996, Crawshaw and Cameron 2000, Park et al. 2006). In the third and final case, anisotropic drying shrinkage of cell wall layers induces internal drying stresses, which can be large enough to damage the wood cell walls (Van den Akker 1961, Kifetew et al. 1998, Thuvander and Berglund 1998, Thuvander et al. 2001). Drying damage is manifested as microcracks irregularly distributed within the cell wall (Wallström and Lindberg 1999, Wallström and Lindberg 2000). Moreover, the NFW content in earlywood significantly increases after drying (Kärenlampi et al. 2005), most likely because of the microscopic drying damage. Changes in wood porosity due to drying may be reversible after rewetting for a prolonged time (Tynjälä and Kärenlampi 2001).

Cell wall porosity in spruce wood after high-temperature drying and rewetting was investigated in terms of thermoporosimetry in Paper VI. The NFW content was predominantly between 20-30 % of the dry wood mass. Recent studies indicate that the NFW content of dried wood specimens is between 30-40 % (Maloney and Paulapuro 1999, Tynjälä and Kärenlampi 2001, Kärenlampi et al. 2005). An obvious explanation for this difference is that these studies have not succeeded in determining correctly the specific heat capacity of the wood specimen. The heat capacity changes along with a thawing process, as described in Section 2.5.1. Previous studies probably indicated overestimated values of heat

capacity, consequently underestimating the amount of melting water, and subsequently overestimating NFW content.

Similar NFW values between earlywood and latewood were found in Paper VI. The same observation had also been reported by Kärenlampi et al. (2005). Those authors, however, found that drying increased the amount of NFW in earlywood. Such a phenomenon was not detected in the present study, possibly due to the reference specimens being stored in a freezer for a few months, which might have induced some freeze-drying.

The greater porosity of earlywood, as compared to latewood, shown in Paper VI may be related to the higher density of pits between fibres (Sirviö and Kärenlampi 1998). Nonetheless the total amount of bound water, *i.e*., water in the cell wall, in earlywood was very high, well exceeding the dry mass of wood. Such a high amount of pore water may be associated to artifacts created during the microtoming of samples. Porosity may also depend on the rewetting time.

The eventual effects of microtoming and rewetting time were investigated by preparing undried earlywood samples with microtomed slices of 60 µm and 200 µm thickness, and keeping them immersed in deionized water for 48 hours before DSC experiments. The results in Paper VI showed that increasing rewetting time opened up pores larger than 145 nm. Moreover, preparing wood slices with a sliding microtome appeared to create new cavities in the cell wall, due to mechanical damage. The thinner the microtomed wood slice, the greater the damage experienced. This effect was most clearly pronounced when examining thin-walled earlywood fibres.

In this study, a pierced aluminium pan was used in the DSC experiments, instead of a sealed pan as used previously (Maloney and Paulapuro 1999, Tynjälä and Kärenlampi 2001, Kärenlampi et al. 2005, Park et al. 2006). This obviously affects the depressed melting temperature of water as a function of pore size. In the case of a pierced pan, the pressure is atmospheric, regardless of temperature, whereas in a sealed pan, the pressure changes as a function of temperature. As the wood sample was placed in the pan at room temperature, lower temperatures within the pan corresponded to lower pressure. Therefore, the melting temperature of water in a sealed pan was slightly higher than that at atmospheric pressure. Consequently, at any depressed melting temperature, the corresponding pore size as given by the Gibbs-Thomson equation (Eq. 13) became underestimated by using a sealed pan. Moreover, the total amount of bound water determined in a sealed pan might be somewhat lower than that determined in a pierced pan, due to some additional pore water eventually melting between -0.1°C and the melting temperature of free water.

According to the International Union of Pure and Applied Chemistry (IUPAC), pores can be classified as micropores (< than 2 nm), mesopores (between 2 and 50 nm) and macropores (> than 50 nm) (Rouquerol et al. 1994). In Paper VI, earlywood sections in all dried specimens contained less bound water than native earlywood, as drying seemed to close macropores over 145 nm. Moreover, the amount of bound water in dried earlywood decreased with increasing drying temperature and time. Apparent closure of macropores may imply the formation of irreversible hydrogen bonds within the cell wall during high-temperature drying, and in particular with extended drying times. Earlywood and latewood sections from specimens slowly dried at 130 °C had the lowest amount of bound water,

regardless of the pore size and despite the fact that these specimens experienced the greatest mass loss during drying. Therefore, pore closure promoted by irreversible hydrogen bonding appeared to dominate over the creation of new cavities by degradation of wood components.

In contrast to the closure of macropores, the amount of mesopores in both earlywood and latewood was almost the same regardless of drying conditions. Kojiro et al. (2010) have also reported that the mesopore volume in wood remains unchanged after heating. However, increasing the heating temperature appears to decrease the amount of micropores, possibly located in the lignin complex (Nakatani et al. 2008, Kojiro et al. 2010). A reduced amount of microcracks, due to stress relaxation, may be partly responsible for the lower amount of bound water found in dried earlywood along with increasing drying temperature and time. In particular, slow drying processes appeared to result in lower NFW content in earlywood. In latewood sections, however, microscopic cell wall damage was less pronounced, and thus the effects of stress relaxation on the cell wall porosity could not be clearly identified.

5. CONCLUSIONS

In this study, heat treatments and high-temperature drying experiments of Norway spruce (*Picea abies*) wood specimens were conducted under different process conditions. The hygroscopicity and the mechanical behaviour of the heat-treated and the high-temperature dried wood were then determined. The pore size distribution within the wood cell wall after drying was further investigated by means of thermoporosimetry. Three mechanisms affecting the structure and properties of heat-treated and high-temperature dried wood were evaluated.

At temperatures beyond 120 °C, the thermal degradation of wood, as indicated by the mass loss, increased with increasing temperature, treatment time and relative humidity in the heating atmosphere. The mass loss was attributed to the degradation of the hemicelluloses, given that these are the least thermally stable polymers of the wood structural components. The higher thermal degradation of wood along with increasing relative humidity appeared to be dependent on the glass transition temperature of the hemicelluloses. In other words, at any temperature, increasing relative humidity in the heating atmosphere had a greater effect on the rate of mass loss if the hemicelluloses were plasticized along with increasing relative humidity.

The hygroscopicity of heat-treated wood decreased with increasing mass loss. This was a direct consequence of mass loss being due to the degradation of the hygroscopic hemicelluloses. However, reduced hygroscopicity of wood was not solely explained by the mass loss, but another mechanism related to the ambient humidity existed. Wood specimens heated at intermediate relative humidity showed about 2 % lower EMC than specimens heated in dry or in water-saturated conditions. As compared to the latter, wood specimens heated at intermediate relative humidity experienced a wetting and high-

temperature drying cycle during the heat-bath treatment. This induced irreversible hydrogen bonding (hornification) within the wood structure, thus reducing the amount of bonding sites available for water sorption. Intermediate relative humidity during a heat-bath treatment would not probably result in reduced hygroscopicity if the relative humidity remained constant during the heat-bath treatment.

The mechanical properties of heat-treated wood were negatively affected by the mass loss. At constant moisture content, the strength, stiffness, ductility and toughness of wood were clearly reduced as compared to untreated wood. The mass loss had a greater impact on strength than on stiffness, the latter allowing a certain extent of mass loss before being reduced. At constant ambient humidity, the mechanical properties of heat-treated wood were higher than at constant moisture content, owing to its lower hygroscopicity. In those circumstances, the strength and stiffness of wood were actually improved up to a mass loss of about 2-3 %. Specimens heated at intermediate relative humidity had the lowest EMC at constant ambient humidity, and thus they exhibited the best mechanical behaviour, which surprisingly included inelastic ductility. Such enhancement in inelastic ductility may be related to hornification. The superior performance of wood heated at intermediate relative humidity could be important for developing artificial ageing processes for wood.

During high-temperature drying, the mass loss and the hornification increased with increasing drying time. The extent of hornification in dried wood was further enhanced with increasing final dryness. Both the mass loss and the hornification resulted in reduced hygroscopicity of wood. Regarding the effects on the mechanical properties, the mass loss and the hornification appeared to compete with each other. However, strength and stiffness results in radial loading were somewhat more sensitive to mass loss than in bending.

Application of slow high-temperature drying to reduce microscopic damage in the wood cell wall did not seem to have a clear effect on the mechanical properties of dried wood. Microscopic drying damage due to anisotropic shrinkage of the cell wall layers is most pronounced in earlywood sections. In longitudinal loading, latewood sections carry most of the total load, not only because of their greater density, but also because they contain a higher portion of the S2 layer, with a small MFA. Consequently, reduction of microscopic damage barely affected the mechanical behaviour of the macroscopic wood structure in bending. In radial loading, the influence of the hemicelluloses in the S1 and S3 layers on the mechanical behaviour of wood is notable. Therefore, any benefits achieved by stress relaxation during slow high-temperature drying processes were offset by the degradation of the hemicelluloses.

Based on these results, drying processes should carefully schedule drying times according to temperature and moisture conditions, in order to avoid significant thermal degradation that would impair the mechanical properties of wood. Moreover, the application of slow high-temperature drying processes, to minimize microscopic cell wall damage, does not provide much benefit regarding the mechanical behaviour of dried wood. Enhancing the mechanical properties of wood may be achieved by conducting a rapid high-temperature drying process up to high dryness. Such a rapid drying process may avoid thermal degradation whilst favouring hornification. Additionally, the occurrence of hornification will result in reduced hygroscopicity, which may not only increase the

mechanical properties of wood, but also improve other physical properties such as dimensional stability.

The pore size distribution in wood, after high-temperature drying followed by rewetting, was investigated by DSC. Earlywood and latewood sections contained a similar amount of micropores. Earlywood, however, showed a greater density of pores larger than 24 nm, with almost twice as much bound water as latewood in macropores of 300-800 nm. The high amount of bound water in earlywood was partially related to the creation of cavities during sample preparation (artifacts). Prolonged rewetting times further increased the amount of bound water in wood.

High-temperature drying appeared to close macropores larger than 145 nm in earlywood, particularly with increasing drying temperature and drying time. The closure of pores by hornification dominated over the creation of cavities by degradation of wood structural components. A somewhat lower NFW content was found in earlywood sections of slowly-dried wood specimens. This was probably due to stress relaxation within the cell wall structure, which reduced the amount of drying microcracks. The NFW content in wood was predominantly between 20-30 % of the dry wood mass, which was lower than previously indicated in the scientific literature. In this study, a new computational method was developed to determine the heat capacity of wood. This computational method appropriately considered the effect of phase change on the heat capacity of water, which had been omitted in previous studies. Nonetheless, further investigations on the pore size distribution in dried earlywood and latewood appear necessary to clearly elucidate the effects of high-temperature drying on the structure of the wood cell wall.

6. REFERENCES

Abe, H., Ohtani, J. & Fukazawa, K. 1992. Microfibrillar orientation of the innermost surface of conifer tracheid walls. IAWA Bulletin 13: 411-417.

Åkerholm, M. & Salmén, L. 2001. Interactions between wood polymers studied by dynamic FT-IR spectroscopy. Polymer 42: 963-969.

— & Salmén, L. 2004. Softening of wood polymers induced by moisture studied by dynamic FTIR spectroscopy. Journal of Applied Polymer Science 94: 2032-2040.

Alén, R. 2000. Structure and chemical composition of wood. In: Stenius, P. (ed.). Forest Products Chemistry. Fapet Oy, Helsinki. p. 12-57.

— , Rytkönen, S. & McKeough, P. 1995. Thermogravimetric behavior of black liquors and their organic constituents. Journal of Analytical and Applied Pyrolysis 31: 1-13.

— , Kuoppala, E. & Oesch, P. 1996. Formation of the main degradation compound groups from wood and its components during pyrolysis. Journal of Analytical and Applied Pyrolysis 36: 137-148.

— , Kotilainen, R. & Zaman, A. 2002. Thermochemical behavior of Norway spruce (*Picea abies*) at 180-225 °C. Wood Science and Technology 36: 163-171.

Andersson, S., Wikberg, H., Pesonen, E., Maunu, S.L. & Serimaa, R. 2004. Studies of crystallinity of Scots pine and Norway spruce cellulose. Trees-Structure and Function 18: 346-353.

Back, E.L. & Salmén, N.L. 1982. Glass transitions of wood components hold implications for molding and pulping processes. Tappi 65: 107–110.

Beall, F.C. & Eickner, H.W. 1970. Thermal degradation of wood components: A review of the literature. Research Paper FPL, USDA Forest Service. 27 p.

Becker, H. & Noack, D. 1968. Studies on dynamic torsional viscoelasticity of wood. Wood Science and Technology 2: 213-230.

Bekhta, P. & Niemz, P. 2003. Effect of high temperature on the change in color, dimensional stability and mechanical properties of spruce wood. Holzforschung 57: 539-546.

Bergander, A. & Salmén, L. 2002. Cell wall properties and their effects on the mechanical properties of fibers. Journal of Materials Science 37: 151-156.

Berlin, E., Kliman, P.G. & Pallansch, M.J. 1970. Changes in state of water in proteinaceous systems. Journal of Colloid and Interface Science 34: 488-494.

Berthold, J., Desbrières, J., Rinaudo, M. & Salmén, L. 1994. Types of adsorbed water in relation to the ionic groups and their counter-ions for some cellulose derivatives. Polymer 35: 5729-5736.

— , Rinaudo, M. & Salmén, L. 1996. Association of water to polar groups; estimations by an adsorption model for ligno-cellulosic materials. Colloids and Surfaces A: Physicochemical and Engineering Aspects 112: 117-129.

Bhuiyan, M.T.R., Hirai, N. & Sobue, N. 2000. Changes of crystallinity in wood cellulose by heat treatment under dried and moist conditions. Journal of Wood Science 46: 431-436.

— & Hirai, N. 2005. Study of crystalline behavior of heat-treated wood cellulose during treatments in water. Journal of Wood Science 51: 42-47.

Bodig, J. & Jayne, B.A. 1993. Mechanics of Wood and Wood Composites. Krieger Publishing Company. 712 p.

Boonstra, M.J., Pizzi, A. & Rigolet, S. 2006. Correlation of ^{13}C-NMR analysis with fungal decay tests of polymeric structural wood constituents I. Basidiomycetes. Journal of Applied Polymer Science 101: 2639-2649.

Borrega, M., Nevalainen, S. & Heräjärvi, H. 2009. Resistance of European and hybrid aspen wood against two brown-rot fungi. Holz als Roh-und Werkstoff 67: 177-182.

Bourgois, J. & Guyonnet, R. 1988. Characterization and analysis of torrefied wood. Wood Science and Technology 22: 143-155.

Brändström, J. 2002. Morphology of Norway spruce tracheids with emphasis on cell wall organization. PhD thesis, Department of Wood Science, Swedish University of Agricultural Sciences. 39 p.

Cave, I.D. 1976. Modelling the structure of the softwood cell wall for computation of mechanical properties. Wood Science and Technology 10: 19-28.

Cousins, W.J. 1978. Young's modulus of hemicellulose as related to moisture content. Wood Science and Technology 12: 161-167.

Crawshaw, J. & Cameron, R.E. 2000. A small angle X-ray scattering study of pore structure in Tencel® cellulose fibres and the effects of physical treatments. Polymer 41: 4691-4698.

Denig, J., Wengert, E.M. & Simpson, W.T. 2000. Drying hardwood lumber. General Technical Report FPL-GTR-118, USDA Forest Service. 138 p.

Duchesne, I., Hult, E., Molin, U., Daniel, G., Iversen, T. & Lennholm, H. 2001. The influence of hemicellulose on fibril aggregation of kraft pulp fibres as revealed by FE-SEM and CP/MAS ^{13}C-NMR. Cellulose 8: 103-111.

Esteves, B., Marques, A.V., Domingos, I. & Pereira, H. 2007. Influence of steam heating on the properties of pine (*Pinus pinaster*) and eucalypt (*Eucalyptus globulus*) wood. Wood Science and Technology 41: 193-207.

— & Pereira, H.M. 2009. Wood modification by heat treatment: a review. BioResources 4: 370-404.

Fahlén, J. & Salmén, L. 2003. Cross-sectional structure of the secondary wall of wood fibers as affected by processing. Journal of Materials Science 38: 119-126.

Feist, W.C. & Sell, J. 1987. Weathering behavior of dimensionally stabilized wood treated by heating under pressure of nitrogen gas. Wood and Fiber Science 19: 183-195.

Fengel, D. & Stoll, M. 1973. On the variation of the cell cross area, the thickness of the cell wall and of the wall layers of sprucewood tracheids within an annual ring. Holzforschung 27: 1-7.

Fengel, D. & Wegener, G. 1989. Wood. Chemistry, Ultrastructure, Reactions. de Gruyter. 613 p.

Fernandes Diniz, J.M.B., Gil, M.H. & Castro, J. 2004. Hornification—its origin and interpretation in wood pulps. Wood Science and Technology 37: 489-494.

Garrote, G., Domínguez, H. & Parajó, J.C. 1999. Hydrothermal processing of lignocellulosic materials. Holz als Roh-und Werkstoff 57: 191-202.

— , Domínguez, H. & Parajó, J.C. 2001. Study on the deacetylation of hemicelluloses during the hydrothermal processing of Eucalyptus wood. Holz als Roh-und Werkstoff 59: 53-59.

Gerhards, C.C. 1982. Effect of moisture content and temperature on the mechanical properties of wood: an analysis of immediate effects. Wood and Fiber Science 14: 4-36.

Giauque, W.F. & Stout, J.W. 1936. The entropy of water and the third law of thermodynamics. The heat capacity of ice from 15 to 273 K. Journal of the American Chemical Society 58: 1144-1150.

Haygreen, J.G. & Bowyer, J.L. 1996. Forest Products and Wood Science. An Introduction. Iowa State University Press. 484 p.

Hietala, S., Maunu, S.L., Sundholm, F., Jämsä, S. & Viitaniemi, P. 2002. Structure of thermally modified wood studied by liquid state NMR measurements. Holzforschung 56: 522-528.

Hill, C. 2006. Wood Modification. Chemical, Thermal and Other Processes. John Wiley & Sons, Ltd. 239 p.

Hillis, W.E. 1984. High temperature and chemical effects on wood stability. Wood Science and Technology 18: 281-293.

Hirosawa, S., Minato, K. & Nakatsubo, F. 2001. Influence of carboxyl group on the acid hydrolysis of cellulose. Journal of Wood Science 47: 141-144.

Homshaw, L.G. 1981. Calorimetric determination of porosity and pore size distribution (PSD): Effect of heat on porosity, pore form, and PSD in water-saturated polyacrylonitrile fibers. Journal of Colloid and Interface Science 84: 127-140.

Irvine, G.M. 1985. The significance of the glass transition of lignin in thermomechanical pulping. Wood Science and Technology 19: 139-149.

Ishikiriyama, K., Todoki, M. & Motomura, K. 1995. Pore size distribution (PSD) measurements of silica gels by means of differential scanning calorimetry I. Optimization for determination of PSD. Journal of Colloid and Interface Science 171: 92-102.

Källander, B. & Bengtsson, C. 2004. High temperature drying of Norway spruce: effects of elevated temperature on wood properties. In: Proceedings of COST E15 Conference on Timber Drying for Value-Added Products, 22nd – 24th April, Athens, Greece. p. 147-156.

Kamdem, D.P., Pizzi, A. & Jermannaud, A. 2002. Durability of heat-treated wood. Holz als Roh-und Werkstoff 60: 1-6.

Kärenlampi, P.P., Tynjälä, P. & Ström, P. 2003a. Molecular reorganization in wood. Mechanics of Materials 35: 1149-1159.

— , Tynjälä, P. & Ström, P. 2003b. Molecular fatigue in steamed wood. International Journal of Fatigue 25: 489-497.

— , Tynjälä, P. & Ström, P. 2005. Phase transformations of wood cell wall water. Journal of Wood Science 51: 118-123.

Kato, K.L. & Cameron, R.E. 1999. A review of the relationship between thermally-accelerated ageing of paper and hornification. Cellulose 6: 23-40.

Kelley, S.S., Rials, T.G. & Glasser, W.G. 1987. Relaxation behaviour of the amorphous behaviour the amorphous components of wood. Journal of Materials Science 22: 617-624.

Kifetew, G., Thuvander, F., Berglund, L. & Lindberg, H. 1998. The effect of drying on wood fracture surfaces from specimens loaded in wet condition. Wood Science and Technology 32: 83-94.

Kim, D.Y., Nishiyama, Y., Wada, M., Kuga, S. & Okano, T. 2001. Thermal decomposition of cellulose crystallites in wood. Holzforschung 55: 521-524.

Kocaefe, D., Chaudhry, B., Poncsak, S., Bouazara, M. & Pichette, A. 2007. Thermogravimetric study of high temperature treatment of aspen: effect of treatment parameters on weight loss and mechanical properties. Journal of Materials Science 42: 854-866.

Kojiro, K., Miki, T., Sugimoto, H., Nakajima, M. & Kanayama, K. 2010. Micropores and mesopores in the cell wall of dry wood. Journal of Wood Science 56: 107-111.

Korkut, S., Kök, M.S., Korkut, D.S. & Gürleyen, T. 2008. The effects of heat treatment on technological properties in Red-bud maple (*Acer trautvetteri* Medw.) wood. Bioresource Technology 99: 1538-1543.

Kubojima, Y., Okano, T. & Ohta, M. 2000. Bending strength and toughness of heat-treated wood. Journal of Wood Science 46: 8-15.

Lawoko, M., Berggren, R., Berthold, F., Henriksson, G. & Gellerstedt, G. 2004. Changes in the lignin-carbohydrate complex in softwood kraft pulp during kraft and oxygen delignification. Holzforschung 58: 603-610.

— , Henriksson, G. & Gellerstedt, G. 2005. Structural differences between the lignin-carbohydrate complexes present in wood and in chemical pulps. Biomacromolecules 6: 3467-3473.

LeVan, S.L. 1989. Thermal degradation. In: Schniewind, A.P. (ed.). Concise Encyclopedia of Wood & Wood-Based Materials. p. 271-273.

Maloney, T.C. & Paulapuro, H. 1999. The formation of pores in the cell wall. Journal of Pulp and Paper Science 25: 430-436.

— & Paulapuro, H. 2001. Thermoporosimetry of pulp fibres. In: Proceedings of 12th Fundamental Research Symposium, Oxford, UK. p. 897-926.

— , Paulapuro, H. & Stenius, P. 1998. Hydration and swelling of pulp fibers measured with differential scanning calorimetry. Nordic Pulp and Paper Research Journal 13: 31-36.

Matsuda, Y., Isogai, A. & Onabe, F. 1994. Effects of thermal and hydrothermal treatments on the reswelling capabilities of pulps and papersheets. Journal of Pulp and Paper Science 20: 323-327.

Matsuo, M., Yokoyama, M., Umemura, K., et al. 2011. Aging of wood: Analysis of color changes during natural aging and heat treatment. Holzforschung 65: 361-368.

Militz, H. 2002. Heat treatment technologies in Europe: scientific background and technological state-of-art. In: Proceedings of Conference on Enhancing the Durability of Lumber and Engineered Wood Products, 11th – 13th February, Kissimmee, Orlando, USA.

Mitchell, P.H. 1988. Irreversible property changes of small loblolly pine specimens heated in air, nitrogen, or oxygen. Wood and Fiber Science 20: 320-335.

Nakamura, K., Hatakeyama, T. & Hatakeyama, H. 1981. Studies on bound water of cellulose by differential scanning calorimetry. Textile Research Journal 51: 607-613.

Nakatani, T., Ishimaru, Y., Iida, I. & Furuta, Y. 2008. Micropore structure of wood: change in micropore structure accompanied by delignification. Journal of Wood Science 54: 252-255.

Nuopponen, M., Wikberg, H., Vuorinen, T., Maunu, S.L., Jämsä, S. & Viitaniemi, P. 2004. Heat-treated softwood exposed to weathering. Journal of Applied Polymer Science 91: 2128-2134.

Obataya, E. 2007. Characteristics of aged wood and Japanese traditional coating technology for wood protection. In: Actes de la journée d'étude Conserver aujourd'hui: les "vieillissements" du bois – Cité de la Musique, 2nd February, France.

Obataya, E., Shibutani, S., Hanata, K. & Doi, S. 2006. Effects of high temperature kiln drying on the practical performances of Japanese cedar wood (*Cryptomeria japonica*) II: Changes in mechanical properties due to heating. Journal of Wood Science 52: 111-114.

O'Sullivan, A.C. 1997. Cellulose: the structure slowly unravels. Cellulose 4: 173-207.

Paakkari, T. & Serimaa, R. 1984. A study of the structure of wood cells by X-ray diffraction. Wood Science and Technology 18: 79-85.

Page, D.H. 1976. A note on the cell-wall structure of softwood tracheids. Wood and Fiber 7: 246-248.

— , El-Hosseiny, F., Winkler, K. & Bain, R. 1972. The mechanical properties of single wood-pulp fibres. Part 1: A new approach. Pulp and Paper Magazine of Canada 73: 72-77.

Park, S., Venditti, R.A., Jameel, H. & Pawlak, J.J. 2006. Changes in pore size distribution during the drying of cellulose fibers as measured by differential scanning calorimetry. Carbohydrate Polymers 66: 97-103.

Passard, J. & Perré, P. 2004. Creep of wood at high temperature: thermal activation or thermal degradation? In: Proceedings of COST E15 Conference on Timber Drying for Value-Added Products, 22nd – 24th April, Athens, Greece. p. 138-146.

Poncsák, S., Kocaefe, D., Bouazara, M. & Pichette, A. 2006. Effect of high temperature treatment on the mechanical properties of birch (*Betula papyrifera*). Wood Science and Technology 40: 647-663.

Pouchlý, J., Biros, J. & Benes, S. 1979. Heat capacities of water swollen hydrophilic polymers above and below 0 °C. Die Makromolekulare Chemie 180: 745-760.

Reiterer, A. & Tschegg, S. 2002. The influence of moisture content on the mode I fracture behaviour of sprucewood. Journal of Materials Science 37: 4487-4491.

Rennie, G.K. & Clifford, J. 1977. Melting of ice in porous solids. Journal of the Chemical Society, Faraday Transactions 1: Physical Chemistry in Condensed Phases 73: 680-689.

Repellin, V. & Guyonnet, R. 2005. Evaluation of heat-treated wood swelling by differential scanning calorimetry in relation to chemical composition. Holzforschung 59: 28-34.

Rouquerol, J., Avnir, D., Fairbridge, C.W., Everett, D.H., Haynes, J.M., Pernicone, N., Ramsay, J.D.F., Sing, K.S.W. & Unger, K.K. 1994. Recommendations for the characterization of porous solids. International Union of Pure and Applied Chemistry 66: 1739-1758.

Sahlberg, U., Salmén, L. & Oscarsson, A. 1997. The fibrillar orientation in the S2-layer of wood fibres as determined by X-ray diffraction analysis. Wood Science and Technology 31: 77-86.

Salmén, L. 1984. Viscoelastic properties of *in situ* lignin under water-saturated conditions. Journal of Materials Science 19: 3090-3096.

Salmén, L. 2004. Micromechanical understanding of the cell-wall structure. Comptes Rendus-Biologies 327: 873-880.

— & Burgert, I. 2009. Cell wall features with regard to mechanical performance. A review. Holzforschung 63: 121-129.

Scallan, A.M. 1977. The accommodation of water within pulp fibres. Fibre-Water Interactions in Paper-Making. Vol. 1. Transactions of the 6th Fundamental Research Symposium, September 1977, Oxford, UK. p. 9-29.

Sirviö, J. & Kärenlampi, P. 1998. Pits as natural irregularities in softwood fibers. Wood and Fiber Science 30: 27-39.

Sivonen, H., Maunu, S.L., Sundholm, F., Jämsä, S. & Viitaniemi, P. 2002. Magnetic resonance studies of thermally modified wood. Holzforschung 56: 648-654.

Sjöström, E. 1981. Wood Chemistry. Fundamentals and Applications. Academic Press, Inc., London. 223 p.

Skaar, C. 1988. Wood-Water Relations. Springer-Verlag. 283 p.

Stamm, A.J. 1956. Thermal degradation of wood and cellulose. Industrial & Engineering Chemistry 48: 413-417.

— , Burr, H.K. & Kline, A.A. 1946. Staybwood-Heat-stabilized wood. Industrial & Engineering Chemistry 38: 630-634.

Stone, J.E. 1955. The rheology of cooked wood. II. Effect of temperature. Tappi 38: 452-459.

— & Scallan, A.M. 1967. The effect of component removal upon the porous structure of the cell wall of wood II. Swelling in water and the fiber saturation point. Tappi 50: 496-501.

Suchy, M., Kontturi, E. & Vuorinen, T. 2010a. Impact of drying on wood ultrastructure: similarities in cell wall alteration between native wood and isolated wood-based fibers. Biomacromolecules 11: 2161-2168.

— , Virtanen, J., Kontturi, E. & Vuorinen, T. 2010b. Impact of drying on wood ultrastructure observed by deuterium exchange and photoacoustic FT-IR spectroscopy. Biomacromolecules 11: 515-520.

Sundqvist, B. 2004. Colour changes and acid formation in wood during heating. PhD thesis, Division of Wood Material Science, Luleå University of Technology. 50 p.

Thuvander, F. & Berglund, L.A. 1998. A multiple fracture test for strain to failure distribution in wood. Wood Science and Technology 32: 227-235.

— , Kifetew, G. & Berglund, L.A. 2002. Modeling of cell wall drying stresses in wood. Wood Science and Technology 36: 241-254.

— , Wallström, L., Berglund, L.A. & Lindberg, K.A.H. 2001. Effects of an impregnation procedure for prevention of wood cell wall damage due to drying. Wood Science and Technology 34: 473-480.

Timell, T.E. 1967. Recent progress in the chemistry of wood hemicelluloses. Wood Science and Technology 1: 45-70.

Tjeerdsma, B.F., Boonstra, M., Pizzi, A., Tekely, P. & Militz, H. 1998. Characterisation of thermally modified wood: molecular reasons for wood performance improvement. Holz als Roh- und Werkstoff 56: 149-153.

— & Militz, H. 2005. Chemical changes in hydrothermal treated wood: FTIR analysis of combined hydrothermal and dry heat-treated wood. Holz als Roh-und Werkstoff 63: 102-111.

Tynjälä, P. & Kärenlampi, P.P. 2001. Spruce cell wall porosity. Variation within annual ring and drying response. In: Proceedings of 1st International Conference of the European Society for Wood Mechanics, 19th – 21st April, Laussane, Switzerland. p. 39-45.

Van den Akker, J.A. 1961. Some theoretical considerations on the mechanical properties of fibrous structures. In. Bolam, F. (ed.). Formation and Structure of Paper. Vol. 1. Transactions of the Symposium held at Oxford, UK, September 1961. p. 205-241.

Vincent, J.F. 1999. From cellulose to cell. Journal of Experimental Biology 202: 3263-3268.

Wallström, L. & Lindberg, K.A.H. 1999. Measurement of cell wall penetration in wood of water-based chemicals using SEM/EDS and STEM/EDS technique. Wood Science and Technology 33: 111-122.

— & Lindberg, K.A.H. 2000. Distribution of added chemicals in the cell walls of high temperature dried and green wood of Swedish pine, *Pinus sylvestris*. Wood Science and Technology 34: 327-336.

Weiland, J.J. & Guyonnet, R. 2003. Study of chemical modifications and fungi degradation of thermally modified wood using DRIFT spectroscopy. Holz als Roh-und Werkstoff 61: 216-220.

Weise, U. 1998. Hornification: mechanisms and terminology. Paperi ja Puu 80: 110-115.

— , Maloney, T. & Paulapuro, H. 1996. Quantification of water in different states of interaction with wood pulp fibres. Cellulose 3: 189-202.

White, R.H. & Dietenberger, M.A. 2001. Wood products: thermal degradation and fire. In: Encyclopedia of Materials: Science and Technology, Elsevier Science, Ltd. p. 9712-9716.

Wikberg, H. & Liisa Maunu, S. 2004. Characterisation of thermally modified hard-and softwoods by ^{13}C CPMAS NMR. Carbohydrate Polymers 58: 461-466.

Williams, M.L., Landel, R.F. & Ferry, J.D. 1955. Temperature dependence of relaxation mechanisms in amorphous polymers and other glassforming liquids. Journal of Applied Physics 77: 3701–3706.

Winandy, J.E. & Lebow, P.K. 2001. Modeling strength loss in wood by chemical composition. Part I. An individual component model for southern pine. Wood and Fiber Science 33: 239-254.

Yan, L. & Zhu, Q. 2003. Direct observation of the main cell wall components of straw by atomic force microscopy. Journal of Applied Polymer Science 88: 2055-2059.

Yasuda, R., Minato, K. & Norimoto, M. 1994. Chemical modification of wood by non-formaldehyde cross-linking reagents. Part 2: Moisture adsorption and creep properties. Wood Science and Technology 28: 209-218.

Young, R.A. 1994. Comparison of the properties of chemical cellulose pulps. Cellulose 1: 107-130.

Zaman, A., Alén, R. & Kotilainen, R. 2000. Thermal behavior of Scots pine (*Pinus sylvestris*) and silver birch (*Betula pendula*) at 200-230 C. Wood and Fiber Science 32: 138-143.